Aminotroponiminates as Ligands for Potential Metal-Based Nitric Oxide Sensors

Katherine J. Franz, Nisha Singh, Bernhard Spingler, and Stephen J. Lippard*

Department of Chemistry, Massachusetts Institute of Technology, Cambridge, Massachusetts 02139

Received March 30, 2000

A family of new fluorescently labeled ligands, H^RDATI, was prepared to develop transition-metal-based NO sensing strategies. The ligands are composed of aminotroponiminates (ATIs) with a dansyl fluorophore on one of the imine nitrogen atoms and an alkyl substituent, either *i*-Pr (**8**), *t*-Bu (**9**), or Bz (**10**), on the other. Bis(chelate) Co^{2+} ([Co($^{i-Pr}$DATI)$_2$] (**12**), [Co($^{t-Bu}$DATI)$_2$] (**14**), [Co(^{Bz}DATI)$_2$] (**15**)) and Zn^{2+} ([Zn($^{i-Pr}$DATI)$_2$] (**13**)) complexes were prepared and characterized by X-ray crystallography. The bis(ATI) complex [Co(*i*-Pr$_2$ATI)$_2$] (**11**) was also prepared and its X-ray crystal structure determined. Cyclic voltammetry reveals reversible redox waves at −2.57 and −0.045 V (vs Cp_2Fe/Cp_2Fe^+) in THF for the Co^{2+}/Co^+ and Co^{3+}/Co^{2+} couples, respectively, of **11**. Only a Co^{2+}/Co^+ wave at −2.09 V is observed for **12**. When excited at 350 nm, the H^RDATI ligands and the diamagnetic Zn^{2+} complex **13** fluoresce around 500 nm, whereas the paramagnetic Co^{2+} complexes quench the fluorescence. These air-stable cobalt compounds react with nitric oxide to dissociate a DATI ligand and form neutral dinitrosyl complexes, [Co(NO)$_2$(^{R}DATI)]. The release of the fluorophore-containing ligand is accompanied by an increase in fluorescence intensity, thus providing a strategy for fluorescent NO sensing. Linking two DATI moieties via a tetramethylene chain affords the ligand H_2DATI-4 (**18**). The Co^{2+} complex [Co(DATI-4)] (**19**) reacts more readily with NO than the bis(DATI) compounds and also displays an increase in fluorescence intensity upon NO binding.

Introduction

Since the discovery in the 1980s that nitric oxide (NO) is the endothelium-derived relaxing factor (EDRF),[1−3] postulated biological roles for NO have continued to proliferate. For example, in addition to cardiovascular signaling, NO also seems to function as a neurotransmitter that may be important in memory and as a weapon to fight infection when released by immune system macrophages.[4] Uncovering these roles and deciphering their implications are complicated by the array of reactions that this gaseous molecule undergoes. In a biological environment, NO can react with a host of targets, including dioxygen, oxygen radicals, thiols, amines, and transition metal ions.[4] Some of the products formed, such as NO_2 and NO^+, are pathophysiological agents, whereas others, such as *S*-nitroso thiols, may in fact themselves be NO-transfer agents.[5] Transition metal centers, especially iron in oxyhemoglobin,[6] can rapidly scavenge free NO, thereby altering the amount available for signaling purposes.

The concentration-dependent lifetime of NO and its ability to diffuse freely through cellular membranes further complicate the delineation of these various processes. With a lifetime of up to 10 min under some conditions[7] and a diffusion range of 100−200 μm for NO,[8] its biological action can be distant from its point of origin. A diffusional spread of 200 μm corresponds to a volume containing approximately 2 million synapses.[9] The development of NO sensors that could monitor the passage of NO through these synapses and around various scavengers is crucial for understanding NO neurochemistry.

A variety of analytical methods are available to monitor aspects of NO in biology, each having its merits and limitations.[10,11] The Griess assay, for instance, is useful for estimating total NO production, but it is not very sensitive, cannot give real-time information, and only measures the stable oxidation product nitrite.[12] Although more sensitive and selective for NO, the chemiluminescent gas-phase reaction of NO with ozone requires purging aqueous samples with an inert gas to strip NO into an analyzer.[13] It too is therefore incapable of monitoring intracellular NO. Electrochemical sensing using microsensors provides in situ real-time detection of NO;[14−16] the only spatial information obtained, however, is directly at the electrode tip and is therefore influenced by the placement of the probe.

These methods and others[10] continue to be invaluable for studying NO-related biochemistry; however, to achieve more detail, new sensors with improved properties are needed. In

(1) Ignarro, L. J. *Angew. Chem., Int. Ed.* **1999**, *38*, 1882−1892.
(2) Furchgott, R. F. *Angew. Chem., Int. Ed.* **1999**, *38*, 1870−1880.
(3) Murad, F. *Angew. Chem., Int. Ed.* **1999**, *38*, 1856−1868.
(4) Pfeiffer, S.; Mayer, B.; Hemmens, B. *Angew. Chem., Int. Ed.* **1999**, *38*, 1714−1731 and references therein.
(5) Jia, L.; Bonaventura, C.; Bonaventura, J.; Stamler, J. S. *Nature* **1996**, *380*, 221−226.
(6) Doyle, M. P.; Hoekstra, J. W. *J. Inorg. Biochem.* **1981**, *14*, 351−358.
(7) Bonner, F. T.; Stedman, G. In *Methods in Nitric Oxide Research*; Feelisch, M., Stamler, J. S., Eds.; John Wiley & Sons: New York, 1996; pp 3−18.
(8) Lancaster, J. R. *Nitric Oxide* **1997**, *1*, 18−30.
(9) Wood, J.; Garthwaite, J. *Neuropharmacology* **1994**, *33*, 1235−1244.
(10) Feelisch, M.; Stamler, J. S. In *Methods in Nitric Oxide Research*; Feelisch, M., Stamler, J. S., Eds.; John Wiley & Sons: New York, 1996; pp 303−307.
(11) *Methods in Enzymology*; Packer, L., Ed.; Academic Press: Boston, MA, 1996; Vol. 268, pp 58−258.
(12) Schmidt, H. H. H. W.; Kelm, M. In *Methods in Nitric Oxide Research*; Feelisch, M., Stamler, J. S., Eds.; John Wiley & Sons: New York, 1996; pp 491−497.
(13) Hampl, V.; Walters, C.; Archer, S. L. In *Methods in Nitric Oxide Research*; Feelisch, M., Stamler, J. S., Eds.; John Wiley & Sons: New York, 1996; pp 309−318.
(14) Malinski, T.; Taha, Z.; Grunfeld, S.; Patton, S.; Kapturczak, M.; Tomboulian, P. *Biochem. Biophys. Res. Commun.* **1993**, *193*, 1076−1082.
(15) Jin, J. Y.; Miwa, T.; Mao, L. Q.; Tu, H. P.; Jin, L. T. *Talanta* **1999**, *48*, 1005−1011.
(16) Trevin, S.; Bedioui, F.; Devynck, J. *Talanta* **1996**, *43*, 303−311.

10.1021/ic000344q CCC: $19.00
Published on Web 08/11/2000

particular, the challenge calls for noninvasive techniques that provide both temporal and spatial data and remain unbiased by the probe itself.

Fluorescence methods are ideally suited to meet these requirements,[17,18] as has been amply demonstrated for sensing intracellular Ca^{2+}.[19,20] Fluorescent NO sensors include DAF (diaminofluorescein)[21−23] and DAN (2,3-diaminonaphthalene),[24] the aromatic vicinal diamines of which react with nitrosating agents (NO^+ or NO_2) to afford fluorescent triazole compounds. DAF compounds can report intracellular NO,[22,23] but their sensing ability relies on NO autoxidation products and not direct detection. A rhodamine-type fluorescent NO indicator similarly senses autoxidation products.[25]

Fluorescent nitric oxide cheletropic traps (FNOCTs) are fluorescent versions of molecules that have been used as EPR spin probes and do react directly with NO.[26,27] The initially formed nitroxide radical species formed are not fluorescent, however. Addition of a common biological reductant such as ascorbic acid is required to reduce the nitroxide and display increased fluorescence intensity.[25,27]

The heme domain in soluble guanylate cyclase (sGC) is an NO receptor for signal transduction and therefore an attractive candidate for biomimetic NO sensors. One approach is to outfit fiber optic probes with fluorescent-dye-labeled heme domains of cytochrome *c*′ [28,29] or sGC.[30] NO reacts with heme domains to change the fluorescence response of the reporter dye, which is ratiometrically measured against standards and gives a linear response selective for NO.[28−30] A quinoline-pendant cyclam has been designed as a fluorescent model of sGC, the quinoline mimicking the distal histidine of sGC and the cyclam representing the porphyrin.[31] The Fe^{2+} center shifts the fluorescence emission of the pendant quinoline, and addition of NO alters the quinoline−Fe interaction, resulting in a *decrease* in fluorescence intensity.[31]

We are interested in harnessing the properties of transition metal−nitrosyl adducts to trigger a *positive* change in fluorescence. Our strategy, recently described in preliminary form,[32] exploits the fluorescence-quenching properties of metal ions with partly filled d shells.[33] In terms of a molecular switch, the paramagnetic metal complexes are therefore in the "off" position. Subsequent addition of the desired analyte displaces a fluorescent ligand from the quenching metal center, thereby turning "on" fluorescence. A similar ligand-dissociation strategy has been employed to monitor pH changes by fluorescence. In this case, a Ni^{2+} cyclam is appended with an alkylamine side chain that is, in turn, linked to an anthracene fragment.[34] Changes in pH affect the binding affinity of the anthracene-tagged amine for the Ni^{2+} center, thereby altering the fluorescence intensity.[34]

Scheme 1

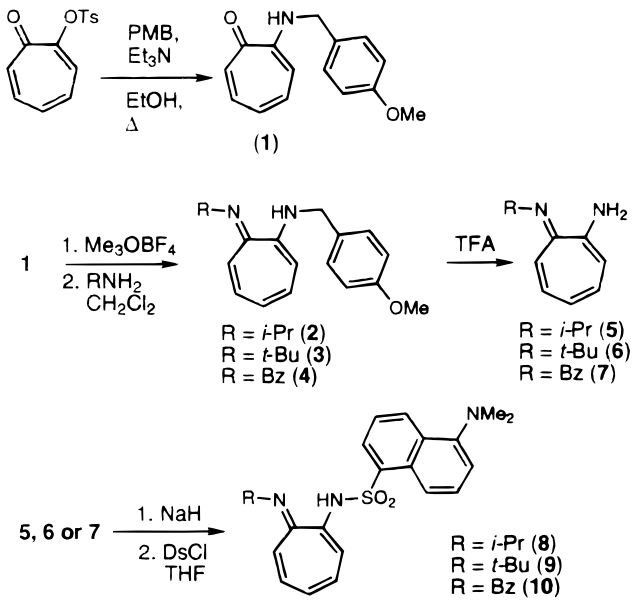

Here we report the syntheses and characterizations of fluorescently labeled aminotroponiminate ligands, H^RDATI and H_2-DATI-4, together with their Zn^{2+} and Co^{2+} complexes. As expected, the Zn^{2+} complexes are fluorescent, whereas the Co^{2+} compounds display only residual emission intensity. The cobalt complexes report the presence of NO by releasing one of their fluorescent moieties upon formation of neutral dinitrosyl species.

Results and Discussion

Syntheses. Scheme 1 outlines the four-step synthetic route that provides gram quantities of H^RDATI ligands in 20−50% yields. These ligands are derived from the N,N′-disubstituted aminotroponimine (HR_2ATI) class of ligands and the dansyl (5-(dimethylamino)naphthalenesulfonamide) fluorophore, widely used for sensor design and labeling of peptides and amino acids.[17] A variety of alkyl substituents can be used to derivatize the ligands; here we chose isopropyl, *tert*-butyl, and benzyl. A methyl-substituted analogue, H^{Me}DATI, was also prepared, but the yield was considerably lower and its metal complexes were not as crystalline as others in the class.

Preparation of the 4-methoxybenzyl (PMB)-protected **1** allows for the asymmetric derivatization of ATI bearing a deactivating tosyl group on one nitrogen atom. Attempts to synthesize *N*-alkyl-2-amino intermediates such as **5**−**7** directly from 2-aminotropolone, which can easily be prepared from 2-(tosyl-

(17) Lakowicz, J. R. *Principles of Fluorescence Spectroscopy*, 2nd ed.; Kluwer Academic/Plenum Publishers: Boston, MA, 1999.
(18) de Silva, A. P.; Gunaratne, H. Q. N.; Gunnlaugsson, T.; Huxley, A. J. M.; McCoy, C. P.; Rademacher, J. T.; Rice, T. E. *Chem. Rev.* **1997**, *97*, 1515−1566.
(19) Minta, A.; Kao, J. P. Y.; Tsien, R. Y. *J. Biol. Chem.* **1989**, *264*, 8171−8178.
(20) Tsien, R. Y. *Biochemistry* **1980**, *19*, 2396−2404.
(21) Kojima, H.; Sakurai, K.; Kikuchi, K.; Kawahara, S.; Kirino, Y.; Nagoshi, H.; Hirata, Y.; Nagano, T. *Chem. Pharm. Bull.* **1998**, *46*, 373−375.
(22) Kojima, H.; Nakatsubo, N.; Kikuchi, K.; Kawahara, S.; Kirino, Y.; Nagoshi, H.; Hirata, Y.; Nagano, T. *Anal. Chem.* **1998**, *70*, 2446−2453.
(23) Kojima, H.; Urano, Y.; Kikuchi, K.; Higuchi, T.; Hirata, Y.; Nagano, T. *Angew. Chem., Int. Ed.* **1999**, *38*, 3209−3212.
(24) Miles, A. M.; Wink, D. A.; Cook, J. C.; Grisham, M. B. In *Methods in Enzymology*; Packer, L., Ed.; Academic Press: Boston, MA, 1996; Vol. 268, pp 105−121 and references therein.
(25) Rieth, R.; Sasamoto, K. *Anal. Commun.* **1998**, *35*, 195−197.
(26) Bätz, M.; Korth, H.-G.; Sustmann, R. *Angew. Chem., Int. Ed. Engl.* **1997**, *36*, 1501−1503.
(27) Meineke, P.; Rauen, U.; de Groot, H.; Korth, H.-G.; Sustmann, R. *Chem.—Eur. J.* **1999**, *5*, 1738−1747.
(28) Barker, S. L. R.; Kopelman, R.; Meyer, T. E.; Cusanovich, M. A. *Anal. Chem.* **1998**, *70*, 971−976.
(29) Barker, S. L. R.; Clark, H. A.; Swallen, S. F.; Kopelman, R.; Tsang, A. W.; Swanson, J. A. *Anal. Chem.* **1999**, *71*, 1767−1772.
(30) Barker, S. L. R.; Zhao, Y.; Marletta, M. A.; Kopelman, R. *Anal. Chem.* **1999**, *71*, 2071−2075.
(31) Katayama, Y.; Takahashi, S.; Maeda, M. *Anal. Chim. Acta* **1998**, *365*, 159−167.
(32) Franz, K. J.; Singh, N.; Lippard, S. J. *Angew Chem., Int. Ed.* **2000**, *39*, 2120−2122.
(33) Bergonzi, R.; Fabbrizzi, L.; Licchelli, M.; Mangano, C. *Coord. Chem. Rev.* **1998**, *170*, 31−46.
(34) Fabbrizzi, L.; Licchelli, M.; Pallavicini, P.; Parodi, L. *Angew. Chem., Int. Ed.* **1998**, *37*, 800−802.

oxy)tropolone and ammonia, resulted in mixtures of products that included significant amounts of the undesired *N,N′*-dialkyl ATI ligands. Protecting one nitrogen with PMB provides a convenient solution to the problem. Activation of the tropolone oxygen of **1** with Me_3OBF_4 followed by reaction with the appropriate alkylamine easily and cleanly affords the *N*-PMB-2-alkyl intermediates **2**−**4**. Cleavage of the methoxybenzyl protecting group with trifluoroacetic acid (TFA) supplies the desired free amino functionality in **5**−**7**. Deprotonation with sodium hydride followed by reaction with dansyl chloride (DNS-Cl) furnishes the final ligands **8**−**10** as yellow-orange powders after purification by flash chromatography.

Moderate yields of the recrystallized metal complexes **11**−**15** are obtained by deprotonating 2 equiv of the ligand with potassium or sodium hydride in THF, followed by addition of anhydrous $CoCl_2$ or $ZnCl_2$. A report of $[Co(R_2ATI)_2]$ compounds with ethyl and aryl substituents claims that the complexes are sensitive to dioxygen and react slowly with some chlorinated solvents.[35] The isopropyl derivative **11** is not oxygen sensitive, nor does it appear to react with chlorinated solvents, although these were limited in use as a precaution. Even though all of the complexes are air stable, they are susceptible to slow hydrolysis by trace moisture, so they were synthesized under a dry nitrogen atmosphere. The complexes are readily soluble in organic solvents such as THF, CH_2Cl_2, and benzene. The DATI complexes are insoluble in diethyl ether and pentane, but [Co(*i*-$Pr_2ATI)_2$] (**11**) is very soluble in diethyl ether.

The synthesis of the linked-DATI ligand **18** follows a route similar to that described above for the H^RDATI ligands. The

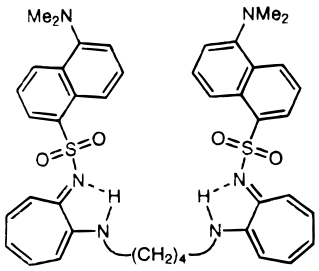

H_2DATI-4 (**18**)

first step involves linking two ATI rings with a polymethylene chain, in a manner analogous to the preparation of the tropocoronand ligands.[36] Activation of "4-dimer-tropolone" with Me_3OBF_4 followed by addition of (4-methoxybenzyl)amine afforded **16** in high yield. Cleaving the 4-methoxybenzyl protecting groups with TFA provided the reactive amine functionalities in **17**. Slow addition of the deprotonated **17** to a solution of excess dansyl chloride at 4 °C gave a modest yield of **18** and suppressed formation of monodansylated product. A slurry of this mustard yellow ligand in THF/CH_3CN became a clear, orange solution after double deprotonation with KH. The use of $[Co(CH_3CN)_4](PF_6)_2$ as the Co source provided the desired monometallic species [Co(DATI-4)] (**19**).

Structural Studies. The molecular structures of **11**, **12**, **14**, and **15** are displayed in Figure 1 as ORTEP diagrams. Single-crystal X-ray diffraction results are provided in Table 1, and selected bond distances and angles are contained in Table 2. A study was also undertaken of one of the free ligands, the *tert*-butyl derivative **9**, an ORTEP diagram of which appears in Figure S1 (Supporting Information). The N−S distance of 1.603(1) Å is slightly shorter than the average N−S distance of 1.623(3) Å in the Co complex **14**. Otherwise, the bond distances and angles are unremarkable and consistent with those in similar sulfonamide ligands.[37]

The synthesis and characterization of [Co(*i*-$Pr_2ATI)_2$] (**11**) permit a comparison between the geometric features of the parent ATI ligand environment and those of the new sulfonamide-appended DATI ligands. The Co^{2+} center in **11** has nearly perfect tetrahedral angles, a common geometry for Co^{2+}.[38] Monoanionic, bidentate ligands often form Co^{3+} octahedral tris(chelate) complexes due to favorable ligand field stabilization.[38] The less bulky methyl-substituted HMe_2ATI ligand prefers such a $[Co(ATI)_3]$ complex, whereas the bulkier diethyl, dibenzyl, and di-*p*-tolyl ATI ligands favor bis(chelate) Co^{2+} species.[35] The syntheses of several $[Co(R_2ATI)_2]$ complexes were reported previously,[35] but not of the isopropyl derivative discussed here. Moreover, no crystal structures of these compounds are available.

The dihedral angle Θ, measured between the planes of the two five-membered chelate rings, is 89.5° in **11**, nearly that of an ideal tetrahedron. The Θ angle measures the degree of twist in related tropocoronand (H_2TC-*n*,*m*) complexes, where two ATI rings are tethered by methylene linker chains of varying lengths (*n*,*m*).[39] The most nearly tetrahedral Θ value, 84.5°, in the series occurs for [Co(TC-6,6)].[39] The average Co−N bond distance of 1.980(3) Å in **11** is quite similar to the value of 1.971(4) Å recorded for [Co(TC-6,6)].[39]

The electron-withdrawing sulfonamide moiety in the DATI ligands slightly affects the Co−N bond lengths by increasing the average distance to 1.999(3) Å in **12**, with similar values for the other derivatives, as shown in Table 2. The coordination chemistry of complexes with sulfonamides is not well developed, but there are some examples of both octahedral[40−42] and tetrahedral[37,43] Co complexes having one or more such ligands. The average Co−N distance revealed in this study is similar to the value of 2.00 Å reported for pseudotetrahedral Co^{2+} complexes of bidentate pyridyl/sulfonamide type ligands.[37,43] A Θ angle of 85° was reported for one of these complexes,[37] which is larger than those in **12**, **14**, and **15**, where Θ = 76.1, 81.4, and 73.8°, respectively. The variations in these values reflect the steric requirements of the different R substituents, isopropyl, *tert*-butyl, and benzyl, respectively. The dansyl groups in **15** are parallel and planar, with an average distance between the ring planes of 3.5(1) Å, a value in the range for $\pi-\pi$ stacking interactions.[44] The dansyl groups are not similarly aligned in the other bis(chelate) structures.

The coordination environment of Zn^{2+} in **13** is also distorted tetrahedral, as shown in Figure S4 (Supporting Information), with Θ = 81.5°. As was found in the Co compounds, the sulfonamide groups lengthen the average Zn−N bond length to 2.01(1) Å, compared with 1.981(3) Å for pseudotetrahedral

(35) Eaton, D. R.; McClellan, W. R.; Weiher, J. F. *Inorg. Chem.* **1968**, *7*, 2040−2046.
(36) Zask, A.; Gonnella, N.; Nakanishi, K.; Turner, C. J.; Imajo, S.; Nozoe, T. *Inorg. Chem.* **1986**, *25*, 3400−3406.
(37) Otter, C. A.; Couchman, S. M.; Jeffery, J. C.; Mann, K. L. V.; Psillakis, E.; Ward, M. D. *Inorg. Chim. Acta* **1998**, *278*, 178−184.
(38) Cotton, F. A.; Wilkinson, G. *Advanced Inorganic Chemistry*, 5th ed.; Wiley-Interscience: New York, 1988; pp 724−741.
(39) Jaynes, B. S.; Doerrer, L. H.; Liu, S.; Lippard, S. J. *Inorg. Chem.* **1995**, *34*, 5735−5744.
(40) Borsari, M.; Menabue, L.; Saladini, M. *J. Chem. Soc., Dalton Trans* **1996**, 4201−4205.
(41) Haider, S. Z.; Malik, K. M. A.; Ahmed, K. J.; Hess, H.; Riffel, H.; Hursthouse, M. B. *Inorg. Chim. Acta* **1983**, *72*, 21−27.
(42) Castresana, J. M.; Elizalde, M. P.; Arrieta, J. M.; Germain, G.; Declerq, J.-P. *Acta Crystallogr., Sect. C* **1984**, *C40*, 763−765.
(43) Uhlig, V. E.; Döring, M. *Z. Anorg. Allg. Chem.* **1982**, *492*, 52−62.
(44) Liu, Z.-H.; Duan, C.-Y.; Hu, J.; You, X.-Z. *Inorg. Chem.* **1999**, *38*, 1719−1724.

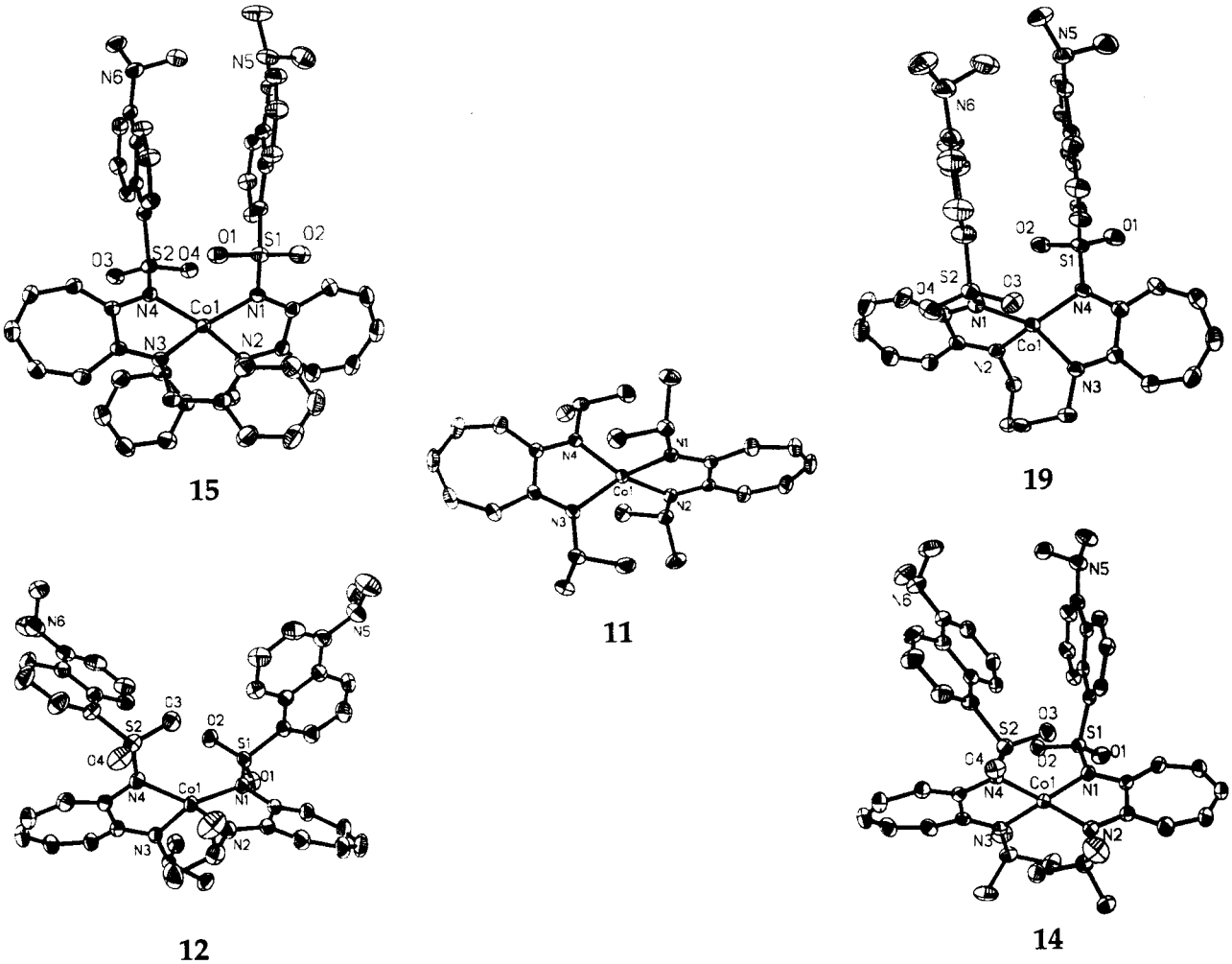

Figure 1. ORTEP diagrams showing selected atom labels and 50% probability ellipsoids for all non-hydrogen atoms of [Co(*i*-Pr$_2$ATI)$_2$] (**11**), [Co($^{i-Pr}$DATI)$_2$] (**12**·CH_2Cl_2), [Co($^{t-Bu}$DATI)$_2$] (**14**·CH_2Cl_2·THF), [Co(^{Bz}DATI)$_2$] (**15**·0.5CH_2Cl_2·0.5THF), and [Co(DATI-4)] (**19**). Solvent molecules are omitted.

Table 1. Summary of X-ray Crystallographic Data

	[Co(*i*-Pr$_2$ATI)$_2$] **11**	[Co($^{i-Pr}$DATI)$_2$] **12**·CH_2Cl_2	[Co($^{t-Bu}$DATI)$_2$] **14**·C_4H_8O·CH_2Cl_2	[Co(^{Bz}DATI)$_2$] **15**·0.5C_4H_8O·0.5CH_2Cl_2
empirical formula	$CoC_{26}H_{38}N_4$	$CoC_{45}H_{48}Cl_2N_6O_4S_2$	$CoC_{51}H_{54}Cl_2N_6O_5S_2$	$CoC_{54.5}H_{48}ClN_6O_{4.5}S_2$
fw	465.53	930.84	1024.95	1052.94
crystal system	triclinic	triclinic	triclinic	orthorhombic
space group	$P\bar{1}$	$P\bar{1}$	$P\bar{1}$	*Pbca*
a (Å)	9.4007(3)	12.1739(2)	13.616(2)	17.3577(5)
b (Å)	10.7556(4)	13.2855(3)	14.060(2)	22.5064(7)
c (Å)	12.9497(5)	14.8238(3)	15.382(2)	25.2381(8)
α (deg)	76.923(1)	102.769(1)	85.40(1)	
β (deg)	76.880(1)	101.401(1)	63.75(1)	
γ (deg)	85.408(1)	94.309(1)	73.341(7)	
V (Å^3)	1241.53(8)	2274.34(8)	2526.4(7)	9859.5(5)
Z	2	2	2	8
ρ_{calcd} (g cm^{-3})	1.245	1.359	1.347	1.371
μ (mm^{-1})	0.711	0.635	0.580	0.541
temp (K)	188(2)	188(2)	188(2)	188(2)
no. of tot. reflns	7736	14 424	16 026	59 920
data/restraints/parameter	5416/0/432	10 060/58/559	11 167/0/604	11 703/102/658
no. of obsd reflns[a]	4835	7829	8809	7733
R1[b]	0.0370	0.0545	0.0404	0.0447
wR2[c]	0.0881	0.1353	0.1111	0.1037
crystal size (mm)	0.30 × 0.20 × 0.12	0.54 × 0.24 × 0.20	0.50 × 0.45 × 0.22	0.40 × 0.30 × 0.15
max/min residuals (eÅ^{-3})	0.273/−0.578	0.840/−0.711	0.516/−0.689	0.562/−0.458

[a] Observation criterion: $I > 2\sigma(I)$. [b] $R1 = \Sigma||F_o| - |F_c||/\Sigma|F_o|$. [c] $wR2 = [\Sigma w(F_o^2 - F_c^2)^2/\Sigma w(F_o^2)^2]^{1/2}$.

[Zn(TC-6,6)].[45] The N−S and S−O bond lengths are comparable to the values found in other 4-coordinate zinc complexes containing sulfonamide ligands.[46−50]

An ORTEP diagram of the linked-DATI Co^{2+} complex **19** is also included in Figure 1, and selected bond distances and angles are contained in Table 2 for comparison with its bis-

Table 2. Selected Bond Distances (Å) and Angles (deg)[a]

	[Co(*i*-Pr_2ATI)$_2$] (**11**)		
Co1−N1	1.981(2)	Co1−N4	1.980(2)
Co1−N2	1.983(2)	Co−N_{ave}	1.980(3)
Co1−N3	1.975(2)		
N1−Co1−N2	81.80(6)	N2−Co1−N4	128.15(6)
N3−Co1−N4	81.66(6)	N1−Co1−N3	121.86(6)
N1−Co1−N4	122.50(6)	Θ	89.5
N2−Co1−N3	126.72(6)		
	[Co($^{i-Pr}$DATI)$_2$] (**12**·CH_2Cl_2)		
Co1−N1	2.001(2)	N1−S1	1.620(2)
Co1−N2	2.000(2)	N4−S2	1.623(2)
Co1−N3	1.999(2)	S1−O1	1.447(2)
Co1−N4	1.995(2)	S1−O2	1.437(2)
Co−N_{ave}	1.999(3)	S2−O3	1.440(2)
		S2−O4	1.439(2)
N1−Co1−N2	80.75(9)	N2−Co1−N4	120.9(1)
N3−Co1−N4	80.33(9)	N1−Co1−N3	120.0(1)
N1−Co1−N4	138.2(1)	Θ	76.1
N2−Co1−N3	122.6(1)		
	[Co($^{t-Bu}$DATI)$_2$] (**14**·CH_2Cl_2·THF)		
Co1−N1	1.977(2)	N1−S1	1.625(2)
Co1−N2	2.014(2)	N4−S2	1.620(2)
Co1−N3	2.005(2)	S1−O1	1.436(2)
Co1−N4	1.980(2)	S1−O2	1.445(2)
Co−N_{ave}	1.99(2)	S2−O3	1.441(2)
		S2−O4	1.445(2)
N1−Co1−N2	80.64(7)	N2−Co1−N4	122.20(7)
N3−Co1−N4	81.03(7)	N1−Co1−N3	125.48(7)
N1−Co1−N4	127.17(7)	Θ	81.4
N2−Co1−N3	126.86(7)		
	[Co(^{Bz}DATI)$_2$] (**15**·0.5CH_2Cl_2·0.5THF)		
Co1−N1	1.986(2)	N1−S1	1.618(2)
Co1−N2	1.998(2)	N4−S2	1.615(2)
Co1−N3	1.990(2)	S1−O1	1.441(2)
Co1−N4	2.008(2)	S1−O2	1.439(2)
Co−N_{ave}	1.99(1)	S2−O3	1.444(2)
		S2−O4	1.446(2)
N1−Co1−N2	80.24(8)	N2−Co1−N4	132.29(8)
N3−Co1−N4	80.39(7)	N1−Co1−N3	133.72(8)
N1−Co1−N4	121.45(8)	Θ	73.8
N2−Co1−N3	116.61(8)		
	[Co(DATI-4)] (**19**)		
Co1−N1	1.986(3)	N1−S2	1.607(3)
Co1−N2	1.963(2)	N4−S1	1.618(3)
Co1−N3	1.996(3)	S1−O1	1.440(2)
Co1−N4	1.977(2)	S1−O2	1.442(2)
Co−N_{ave}	1.98(1)	S2−O3	1.439(2)
		S2−O4	1.437(2)
N1−Co1−N2	79.78(10)	N2−Co1−N4	136.82(10)
N3−Co1−N4	79.93(10)	N1−Co1−N3	141.36(11)
N1−Co1−N4	123.78(10)	Θ	62.2
N2−Co1−N3	103.94(10)		

[a] Numbers in parentheses are estimated standard deviations of the last significant figures. Atoms are labeled as indicated in Figure 1. The angle Θ is the dihedral angle between the planes of the two five-membered chelate rings.

(chelate) relatives. The Co^{2+} center has distorted tetrahedral geometry, with Θ = 62.2°. The tetramethylene linker chain restricts the N2−Co1−N3 angle to 103.94(10)°, very similar to the 102.1(1)° angle observed in the related macrocyclic tropocoronand compound [Co(TC-4,4)].[39] The opposing angle N1−Co−N4, however, is not restrained in **19** and opens to 123.78(10)°, larger than the restrained 101.3(1)° angle in [Co(TC-4,4)].[39] Similar to those in **15** described above, the dansyl groups in **19** also align in a parallel−planar fashion, with the two six-membered aromatic rings attached at the S atoms

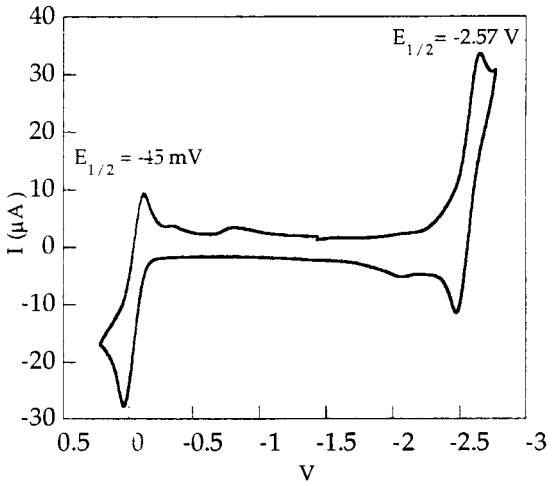

Figure 2. Cyclic voltammogram of [Co(*i*-Pr_2ATI)$_2$] (**11**) in THF with 0.5 M (*n*-Bu_4N)(ClO_4) at a scan speed of 100 mV/s. Potentials are reported vs Cp_2Fe/Cp_2Fe^+.

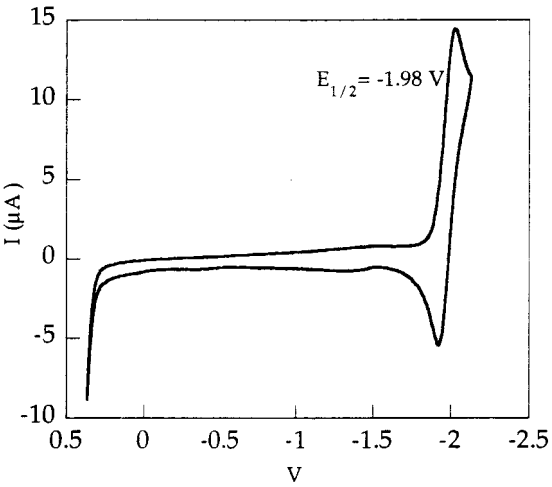

Figure 3. Cyclic voltammogram of [Co(^{Bz}DATI)$_2$] (**15**) in THF with 0.5 M (*n*-Bu_4N)(ClO_4) at a scan speed of 100 mV/s. Potentials are reported vs Cp_2Fe^+/Cp_2Fe.

stacked at an average aryl−aryl distance of 3.63(9) Å. The average Co−N bond distance of 1.98(1) Å is similar to the values for the [Co(^{R}DATI)$_2$] compounds but longer than the value of 1.88(2) Å found in [Co(TC-4,4)],[39] consistent with the electron-withdrawing properties of the sulfonamide functionality.

Electrochemistry. Representative cyclic voltammograms of [Co(*i*-Pr_2ATI)$_2$] (**11**) and [Co(^{Bz}DATI)$_2$] (**15**) are shown in Figures 2 and 3, respectively. Half-wave potentials for these compounds are presented in Table 3, along with values recorded for **12**, **13**, and a series of [Co(TC-*n*,*m*)] compounds. Compound **11** displays a reversible oxidation at −0.045 V and a reversible reduction at −2.57 V in THF versus Cp_2Fe/Cp_2Fe^+. These potentials describe a Co^{2+} compound that is more difficult both

(45) Doerrer, L. H.; Lippard, S. J. *Inorg. Chem.* **1997**, *36*, 2554−2563.
(46) Romero, J.; García-Vásquez, J. A.; Durán, M. L.; Castiñeiras, A.; Sousa, A.; Garnovskii, A. D.; Garnovskii, D. A. *Acta Chem. Scand.* **1997**, *51*, 672−675.
(47) Quinzani, O. V.; Tarulli, S.; Piro, O. E.; Baran, E. J.; Castellano, E. E. *Z. Naturforsch. B* **1997**, *52*, 183−187.
(48) Baenziger, N. C.; Modak, S. L.; Fox, C. L. J. *Acta Crystallogr., Sect. C* **1983**, *C39*, 1620−1623.
(49) Denmark, S. E.; O'Conner, S. P.; Wilson, S. R. *Angew. Chem., Int. Ed.* **1998**, *37*, 1149−1151.
(50) Koike, T.; Kimura, E.; Nakamura, I.; Hashimoto, Y.; Shiro, M. *J. Am. Chem. Soc.* **1992**, *114*, 7338−7345.

Table 3. Cyclic Voltammetric Data[a]

complex	Co^{2+}/Co^{+}	Co^{3+}/Co^{2+}	E_{p_a}[d]
[Co(TC-3,3)][b]	−2.12	−0.49	0.49[c]
[Co(TC-4,4)]	−2.22	−0.41	0.54[c]
[Co(TC-4,5)]	−2.35	−0.38	0.52[c]
[Co(TC-5,5)]	−2.40	−0.24	0.49[c]
[Co(TC-6,6)]	−2.46	−0.26	0.55[c]
[Co(*i*-Pr_2ATI)$_2$] (**11**)	−2.57	−0.045	
[Co(^{Bz}DATI)$_2$] (**15**)	−1.98		0.47, 0.73, 1.08[c]
[Co($^{i-Pr}$DATI)$_2$] (**12**)	−2.09		0.47, 0.84, 1.06
[Zn($^{i-Pr}$DATI)$_2$] (**13**)			0.47, 0.93

[a] All potentials are given in volts and referenced to Cp_2Fe/Cp_2Fe^+ at 0.0 V. Data were recorded for THF solutions unless otherwise noted. [b] Results for all [Co(TC-*n*,*m*)] compounds are taken from ref 51. [c] CH_2Cl_2. [d] E_{p_a} refers to an irreversible process.

to oxidize and to reduce than its macrocyclic analogue [Co(TC-6,6)], for which the values are −0.26 and −2.46 V, respectively. This observation continues a trend established in the tropocoronand series that compounds with higher Θ values are more difficult both to oxidize and to reduce.[51]

The [Co(^{R}DATI)$_2$] compounds have only one quasi-reversible wave, that for a reduction, as displayed in Figure 3 for the benzyl derivative **15**. The Co^{2+}/Co^{+} half-wave potential occurs at −2.0 V for **12** and **15**. This value is significantly more positive than that found for **11**. An irreversible wave at 0.47 V was confirmed to be that for ligand oxidation, not a metal-centered process, by observation of a similar wave for the Zn complex **13**. At least two other irreversible processes occur for **12** and **15**, as indicated in Table 3; for **12**, the half-wave potentials are 0.47, 0.84, and 1.06 V. Complexes of the chelating ligand 2-(2-*p*-toluenesulfonamido)pyridine also give similar irreversible electrochemical oxidations, believed to be ligand based, at 0.51, 0.74, and 0.96 V versus Cp_2Fe/Cp_2Fe^+.[37] The Co^{2+}/Co^{3+} couple must therefore occur at a potential more positive than 0.47 V but is unobservable. The DATI complexes are thus easier to reduce and more difficult to oxidize than their parent ATI and TC-*n*,*m* compounds, a property that is consistent with the electron-withdrawing environment provided by the sulfonamide functionality.

Fluorescence. When excited at 350 nm, ligand **8** displays a broad emission band centered around 500 nm due to the dansyl fluorophore. A plot of concentration versus fluorescence intensity (Figure S7, Supporting Information) reveals that the optimal emission intensity occurs at 50 μM. At higher concentrations, the intensity decreases because of inner filter effects.[17] Plots for the Zn complex are shown in Figure S8 (Supporting Information) and show a similar optimal concentration range. The chelated Zn^{2+} complex **13** does not shift the emission wavelength, $\lambda_{max} = 506$ cm^{-1}, compared with that of the free ligand. This result contrasts with the blue shift of about 25 cm^{-1} observed upon zinc complexation by a dansyl-pendant cyclen ligand.[52]

Complexation of ligands **8**, **9**, and **10** by Co^{2+} results in significant fluorescence quenching. Solutions of 40 μM **12**, **14**, and **15** in CH_2Cl_2 display only 5−6% of the fluorescence intensity of the free ligands, as illustrated in Figure 4 for **12**. Fluorescence quenching by transition metals can occur by energy or electron transfer between the excited state of the fluorophore and empty or partially filled d orbitals on the metal.[33] The Co^{2+} ion therefore provides an efficient pathway for quenching the fluorescence of the DATI ligands, whereas the filled d-shell Zn^{2+} ion remains fluorescent.

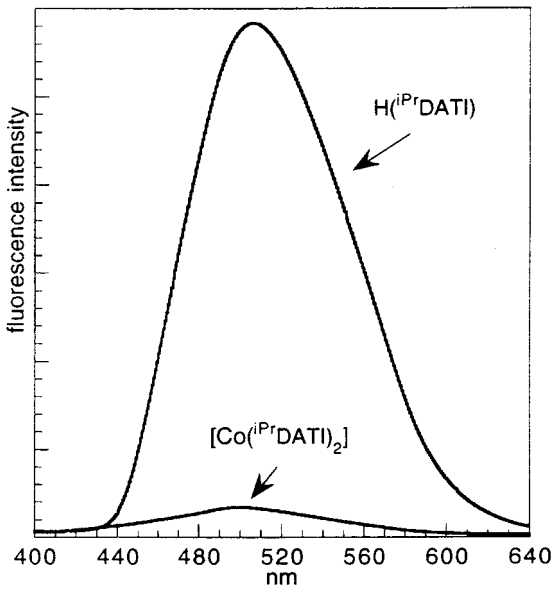

Figure 4. Comparison of the fluorescence emission spectra of 46 μM CH_2Cl_2 solutions of H^{i-Pr}DATI (**8**) and [Co($^{i-Pr}$DATI)$_2$] (**12**). Excitation = 350 nm.

NO Reactivity of [Co(^{R}DATI)$_2$]. The reactions of **12**, **14**, and **15** in CH_2Cl_2 solutions with NO are slow, but after several hours of exposure to an NO atmosphere, two new bands appear at 1838 and 1760 cm^{-1} in the IR spectrum of **20a**. For **20b** and **20c**, the corresponding values are 1833, 1760 cm^{-1} and 1833, 1755 cm^{-1}, respectively. The appearance of these NO stretching bands indicates the formation of dinitrosyl complexes, examples of which display symmetric and asymmetric stretching modes between 1750−1798 and 1820−1876 cm^{-1}.[53−60]

In addition to the similarity of our ν_{NO} bands to those in these examples, they are suggestive of those at 1809 and 1730 cm^{-1} for the nondansylated parent complex, [Co(NO)$_2$(*i*-Pr_2ATI)] (**21**). The shift to higher energy in the spectra of **20a**−**c** is expected owing to the electron-withdrawing sulfonamides of the DATI ligands. Although we were unable to obtain crystal structures of **20a**−**c**, the structure of the related molecule [Co(NO)$_2$(*i*-Pr_2ATI)][61] strongly suggests that the geometries of **20a**−**c** will be pseudotetrahedral. Because of the lack of appreciable reactivity differences across the series of [Co(^{R}DATI)$_2$] compounds, we chose to focus on [Co($^{i-Pr}$DATI)$_2$] (**12**) for further studies.

The ^{1}H NMR spectrum of paramagnetic **12** reveals broad but well-defined resonances at 92.3, 87.2, 14.3, −1.3, −36.7, −74.2,

(51) (a) Doerrer, L. H.; Bautista, M. T.; Lippard, S. J. *Inorg. Chem.* **1997**, *36*, 3578−3579. (b) Doerrer, L. H. Ph.D. Dissertation, Massachusetts Institute of Technology, 1997.
(52) Koike, T.; Watanabe, T.; Aoki, S.; Kimura, E.; Shiro, M. *J. Am. Chem. Soc.* **1996**, *118*, 12696−12703.
(53) Field, J. S.; Wheatley, P. J.; Bhaduri, S. *J. Chem. Soc., Dalton Trans.* **1974**, 74−79.
(54) Haymore, B. L.; Huffman, J. C.; Butler, N. E. *Inorg. Chem.* **1983**, *22*, 168−170.
(55) Kaduk, J. A.; Ibers, J. A. *Inorg. Chem.* **1977**, *16*, 3283−3287.
(56) Reichert, B. E. *Acta Crystallogr., Sect. B* **1976**, *B32*, 1934−1936.
(57) Roustan, J.-L.; Ansari, N.; Le Page, Y.; Charland, J.-P. *Can. J. Chem.* **1992**, *70*, 1650−1657.
(58) Aresta, M.; Ballivet-Tkatchenko, D.; Bonnet, M. C.; Faure, R.; Loiseleur, H. *J. Am. Chem. Soc.* **1985**, *107*, 2994−2995.
(59) Hendrickson, A. R.; Ho, R. K. Y.; Martin, R. L. *Inorg. Chem.* **1974**, *13*, 1279−1281.
(60) Martin, R. L.; Taylor, D. *Inorg. Chem.* **1976**, *15*, 2970−2977.
(61) The pseudotetrahedral dinitrosyl structure of **21** was determined in space group *Iba*2 with $a = 13.711(2)$ Å, $b = 24.639(6)$ Å, $c = 8.997(2)$ Å, $V = 3039.4(11)$ Å^3, $Z = 8$, $T = 188(2)$ K, R1 = 0.125, wR2 = 0.227. The crystal quality precluded better refinement of the structure.

and −91.7 ppm in C_6D_6. By comparison with reported spectra of $[Co(R_2ATI)_2]$ complexes, we assign the 87.2, −91.7, and 92.3 ppm resonances to the α, *β*, and *γ* tropolone ring protons, respectively.[35] In the presence of NO, these peaks are replaced by two sets of resonances in positions expected for diamagnetic compounds. One set of signals corresponds to the spectrum of the free ligand H^{i-Pr}DATI, and the other is consistent with the dinitrosyl−mono(DATI) formulation assigned to **20a** (eq 1). The

$$\underset{\mathbf{12}}{[Co(^{i-Pr}DATI)_2]} \xrightarrow[e^-,\,H^+]{NO} \underset{\mathbf{20a}}{[Co(NO)_2(^{i-Pr}DATI)]} + H^{i-Pr}DATI \quad (1)$$

reaction was slow, but after 4 days, **20a** and H^{i-Pr}DATI formed in a 1:1 ratio. The yield (75%) was calculated by comparing peak integrations of the products against those of acetone added as an internal standard. A small amount of **12** was still present in the solution. The source of the protons was assumed to be adventitious water in the solvent. Addition of 1 equiv of water helped to drive the reaction to completion, as evidenced by increased intensity of the ν_{NO} bands in the IR spectrum after shorter reaction times when wet solvent was used. Similar reactivity was observed during the reaction of $[Co(i\text{-}Pr_2ATI)_2]$ with NO, the formation of the dinitrosyl compound **21** coinciding with the release of the free ligand H-*i*-Pr$_2$ATI. Unlike the case for the DATI compounds, this reaction proceeded within minutes rather than hours and the product was not stable under excess NO.

Known cobalt dinitrosyl complexes are 4-coordinate, pseudotetrahedral species designated as $\{Co(NO)_2\}^{10}$ in the Enemark−Feltham notation for metal nitrosyl compounds. In this notation, *n* (10 in this case) denotes the number of electrons in the $\{MNO\}^n$ unit as the sum of the d electrons of the metal plus the electrons in π^* orbitals of NO.[62] By formal count, a Co^{2+} species such as **12** would bind two molecules of NO to give *n* = 9, not 10, d electrons. In some reported examples, $\{Co(NO)_2\}^{10}$ forms from Co^{2+} starting materials, the metal center providing the needed electron by disproportionation of $[Co^{II}L_2]$ to give $[Co^{I}(NO)_2L]$ and $[Co^{III}L_3]$.[59,60,63] Owing to the steric bulk of the DATI ligands, it is unlikely that tris(chelate) Co^{3+} complexes could form. The ^{1}H NMR spectrum of the reaction mixture of **12** and NO discussed above reveals only two new species, which together account for at least 75% of the starting material. Unreacted starting material comprises another fraction, eliminating the possibility of a Co^{3+} byproduct in the reaction. Although the nature of the reductant remains unknown, reductive nitrosylation is well documented.[64]

Fluorescence Response of [Co($^{i-Pr}$DATI)$_2$] (12) + NO. As expected from the unfilled d shell of the Co^{2+} starting complex,[33] the fluorescence of the DATI ligands is quenched in **12**. The dissociation of a fluorescent ligand upon NO binding to the Co center, however, provides a mechanism for sensing NO. As shown in Figure 5, a CH_2Cl_2 solution of **12** displays a slow but steady increase in emission at 505 nm in the presence of NO. After 6 h, the fluorescence intensity increases by approximately 8-fold over that of the starting complex.

This 8-fold increase in the presence of NO contrasts sharply with the lack of response when **12** is exposed to air (data not shown). The Co^{2+} complexes are remarkably air stable, both in solution and in the solid state. Although **12**, **14**, and **15** are

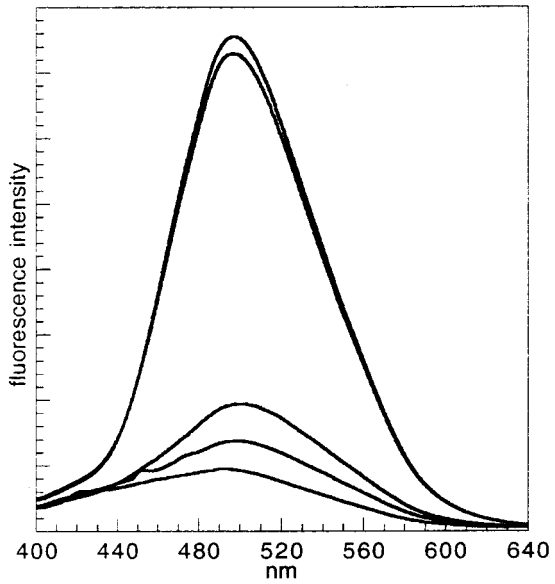

Figure 5. Emission spectra of a 45 μM CH_2Cl_2 solution of [Co($^{i-Pr}$DATI)$_2$] (**12**) after exposure to NO gas. The lowest intensity trace is that of **12** in an N_2 atmosphere, excited at 350 nm. The other spectra were recorded, in increasing order of intensity, 5 min, 3 h, 4.5 h, and 6 h after addition of NO gas to the headspace of the sample cell. About an 8-fold increase in intensity was observed from that of the starting material. A control cell that was exposed to air over the same periods of time showed no change its fluorescence emission.

O_2 stable, they do not tolerate moisture and will slowly hydrolyze if solutions are exposed to air for too long a period of time (several days). They are similarly sensitive to the addition of protons from other sources. Figure S9 (Supporting Information) shows the fluorescence response of a CH_2Cl_2 solution of **12** following the addition of 2 equiv of HBAr′$_4$·2Et$_2$O. The response is similar to that given in Figure 5 after the addition of NO but reaches an 8-fold increase in half the time.

To test the hypothesis that liberation of free ligand in the reaction of **12** with NO accompanies the positive fluorescence response, emission spectra of **12** were recorded after incremental additions of a solution of H^{i-Pr}DATI (Figure S10, Supporting Information). As expected, the emission at 505 nm increases with increasing amounts of added free ligand. The most intense emission recorded occurs when approximately 1 equiv of ligand is added to the cobalt complex, giving a 5−6-fold increase in fluorescence over that of **12** alone. The Co^{2+} center therefore does not exert a quenching effect on other fluorophores in solution but only affects the fluorophore to which it is ligated. Since the intensity increase seen here is comparable to the changes observed after addition of NO to **12**, it is reasonable to conclude that the amount of H^{i-Pr}DATI formed in the NO reaction is sufficient to elicit the fluorescence response observed in Figure 5. The key event responsible for the fluorescence enhancement, therefore, is dissociation of a fluorophore-containing ligand upon formation of the metal−nitrosyl adduct.

It is also possible that the dinitrosyl **20a** itself may contribute to the fluorescence response. Empty or partially filled d orbitals of a metal provide an efficient energy-transfer-quenching pathway for excited-state fluorophores.[33] Metal ions with filled d shells, such as Zn^{2+} or Cu^{+}, do not provide such an energy-transfer pathway, and fluorescence can occur.[65] The compound [Zn($^{i-Pr}$DATI)$_2$] is one such example. Formation of a diamagnetic $\{Co(NO)_2\}^{10}$ moiety may also remove a fluorescence-quenching pathway.

(62) Enemark, J. H.; Feltham, R. D. *Coord. Chem. Rev.* **1974**, *13*, 339−406.
(63) Del Zotto, A.; Mezzetti, A.; Rigo, P. *Inorg. Chim. Acta* **1990**, *171*, 61−69.
(64) Scheidt, W. R.; Ellison, M. K. *Acc. Chem. Res.* **1999**, *32*, 350−359.
(65) Fabbrizzi, L.; Licchelli, M.; Pallavicini, P. *Acc. Chem. Res.* **1999**, *32*, 846−853.

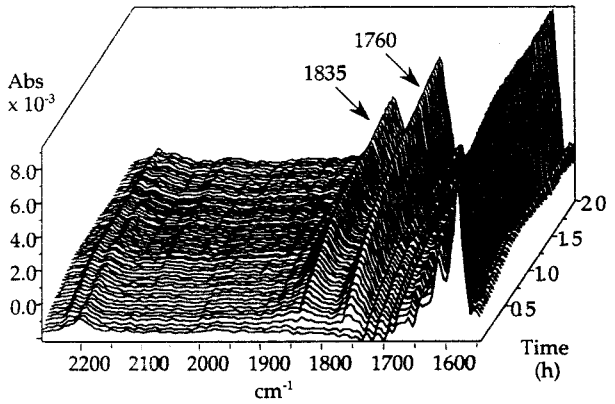

Figure 6. In situ IR reaction spectra of [Co(DATI-4)] (**19**) in CH_2Cl_2 at room temperature as NO gas was introduced into the headspace of the reaction flask. The bands at 1837 and 1760 cm^{-1} indicate the development of a dinitrosyl species. A residual amount of N_2O is observed at 2223 cm^{-1} (band not labeled), but this band does not grow in to an appreciable intensity. The reaction was monitored for 20 h, but no significant changes were observed after the 2 h period represented in this figure.

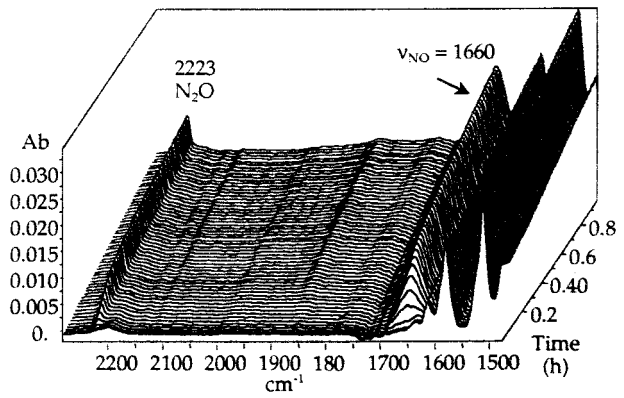

Figure 7. In situ IR reaction spectra of [Co(DATI-4)] (**19**) in CH_2Cl_2 at −78 °C as NO gas was introduced into the headspace of the reaction flask. The growth of a nitrosyl stretch at 1660 cm^{-1} tracks the formation of N_2O at 2223 cm^{-1}. Both bands maximize within 20 min and then are stable at -78 °C for the remainder of the monitoring time, slightly more than 1 h. The cold bath was then removed. As the reaction mixture warmed to room temperature, the band at 1660 cm^{-1} was replaced by bands at 1837 and 1760 cm^{-1}, and the reaction spectra (not shown) appeared analogous to those displayed in Figure 6.

NO Reactivity of [Co(DATI-4)] (19). The NO-induced fluorophore dissociation observed upon the reaction of **12** with NO led to the design and synthesis of a linked-DATI ligand. In this construct, one arm of the ligand can dissociate from the metal center but remain part of the complex. Such a strategy could possibly facilitate a reversible NO-binding complex. The reaction of **19** with NO proceeds 50 times faster than that of compounds **12**, **14**, and **15**, perhaps due to geometric differences. The linker chain in **19** imposes some distortion at the metal center, forcing it even further away from an idealized tetrahedral environment compared to those of **12**, **14**, and **15**. NO may therefore have better access to the metal center in **19**, and release of the strain would drive the Co center to adopt a more favorable pseudotetrahedral geometry.

The faster reaction time made **19** amenable to in situ IR monitoring of its reaction with NO. Figure 6 displays the changes seen in the NO stretching frequency region when a CH_2Cl_2 solution of **19** at room temperature was anaerobically exposed to a stream of NO gas. Two new bands appeared at 1835 and 1760 cm^{-1}, very closely matching the signature frequencies of **20b** at 1833 and 1760 cm^{-1}. The formation of these characteristic bands indicates formation of a Co dinitrosyl compound that has an environment almost identical to that of **20b**. In the solid state, these bands appear at 1827 and 1751 cm^{-1} and shift to 1793 and 1719 cm^{-1} upon isotopic labeling with ^{15}NO, in agreement with the values 1794 and 1720 cm^{-1} calculated by assuming a classic diatomic oscillator model.

When the reaction of **19** with NO was followed at −78 °C, however, new bands at 1660 and 2223 cm^{-1} appeared simultaneously, as displayed in Figure 7. Both bands reached their maximum intensity in about 15 min, after which they remained stable at −78 °C for at least 45 min. When the reaction mixture was warmed to ambient temperature, the 1660 cm^{-1} signal disappeared and the characteristic dinitrosyl bands at 1835 and 1760 cm^{-1} appeared (not shown). Cooling the solution back to −78 °C did not cause the 1660 cm^{-1} band to return.

The band at 2223 cm^{-1} is the signature of N_2O and was also observed during NO disproportionation reactivity by Mn and Fe tropocoronand complexes.[66,67] In both of these cases, the first step in the reaction with NO was formation of a mononitrosyl adduct. It is possible that the band at 1660 cm^{-1} corresponds to a 5-coordinate mononitrosyl species that is stable at low temperature and upon warming decays to a $\{Co(NO)_2\}^{10}$

Scheme 2

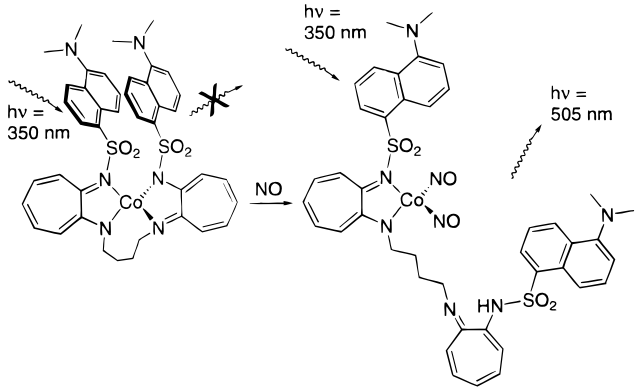

product. Once the stable, tetrahedral dinitrosyl adduct forms, it does not react further with NO or NO-derived species.

To obtain a pseudotetrahedral coordination environment, one of the DATI arms must dissociate from the metal center, as shown in Scheme 2. The ^1H NMR spectrum of the reaction mixture of **19** and NO is difficult to interpret because of extensive signal overlap, but it clearly contains only diamagnetic signals and the methyl proton resonances of the dansyl group are no longer equivalent, as they are in the spectrum of ligand **18**.

Fluorescence Response of [Co(DATI-4)] (19) + NO. As was the case for the $[Co(^RDATI)_2]$ compounds, the Co^{2+} center in **19** quenches the fluorescence of the DATI-4 fluorophore. Under an NO atmosphere, a solution of **19** rapidly displays an increase in fluorescence at 505 nm, however, as shown in Figure 8. The first emission spectrum shown in Figure 8a is that of the starting compound **19**. The next spectrum was recorded 3 min after NO addition, by which time the emission intensity had already doubled. The response continued to rise over the course of several hours, affording a greater than 4-fold increase in fluorescence intensity compared to that of the starting material. The initial response is much faster than those for the

(66) Franz, K. J.; Lippard, S. J. *J. Am. Chem. Soc.* **1998**, *120*, 9034−9040.
(67) Franz, K. J.; Lippard, S. J. *J. Am. Chem. Soc.* **1999**, *121*, 10504−10512.

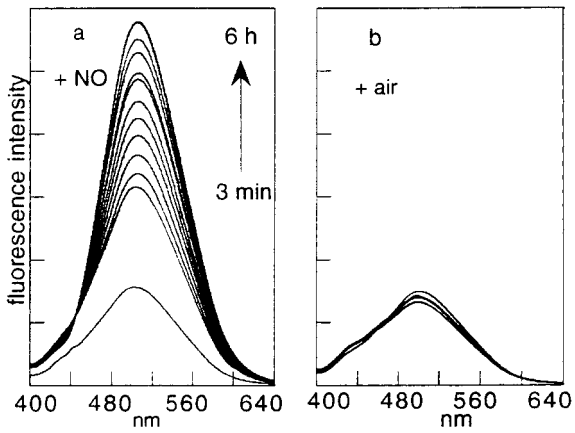

Figure 8. (a) Fluorescence emission spectra showing the increase in intensity at 505 nm (excitation = 350 nm) when a 40 μM CH_2Cl_2 solution of [Co(DATI-4)] (**19**) was exposed to 1 atm of NO gas. The lowest intensity spectrum is that of the starting material; the next spectrum was recorded 3 min after addition of NO to the headspace. After 6 h (top spectrum), a greater than 4-fold increase in intensity over that of the starting material was observed. (b) Fluorescence emission spectra of a 40 μM CH_2Cl_2 solution of **19**, unaffected by exposure to air over a period of 6 h.

analogous reactions with the first-generation [Co(^{R}DATI)$_2$] compounds, which only show appreciable increases after several hours.

To estimate the sensitivity of **19**, aliquots of NO gas were injected into 2 mL of a 35 μM CH_2Cl_2 solution of **19** at 25 °C. Addition of 2 μL of NO caused only a slight fluorescence enhancement, whereas addition of 5 μL of NO doubled the fluorescence intensity within 1 h (Figure S11, Supporting Information). These results place the detection limit of **19** at 50−100 μM, a value that needs to be lowered for biological applications.

Creation of a slightly strained geometry at the Co center by linking the DATI ligands does not jeopardize the air stability of **19**. Figure 8b demonstrates the lack of a fluorescence response when **19** is exposed to air. In the solid state and in solution, **19** appears to be stable to O_2 indefinitely. The concentration of NO involved in regulatory functions such as vasodilation and neurotransmission is estimated to be 0.1−10 μM.[7] Because the reaction of NO with O_2 to form NO_2 is second order in [NO], the lifetime of NO at these functional concentrations can be up to 10 min in an aerobic environment.[7] Sensors that react with O_2 to give a fluorescence response are therefore of limited value for these applications.

Summary and Conclusions

A new route to asymmetrically derivatized aminotroponiminate ligands has been developed. Protecting one of the imino nitrogens with a 4-methoxybenzyl group provides a facile and general way to functionalize the ATI core with a sulfonamide group, specifically a dansyl fluorophore. This synthetic route provides a new family of fluorescent ligands for development as potential NO sensors. As anticipated, the filled d-shell Zn^{2+} complex remains fluorescent, whereas Co^{2+} quenches fluorescence of the DATI ligands.

The [Co(DATI)$_2$] compounds **12**, **14**, and **15** represent our initial attempts at developing metal-based, fluorescent NO sensors. These molecules address one of the inherent challenges of designing an NO sensor, namely, discrimination of NO over O_2. The complexes are indefinitely dioxygen stable and display significantly enhanced fluorescence in the presence of NO. The sensing behavior of [Co(DATI)$_2$] results from the dissociation of one DATI ligand upon coordination of two nitrosyl ligands to the metal center. Removal of a fluorophore from the quenching metal center revives fluorescence, thereby reporting the presence of NO. An additional contribution to the fluorescence enhancement may come from DATI bound to the dinitrosylmetal center itself, which has been characterized as {Co(NO)$_2$}^{10}.

The linked-DATI ligand DATI-4 represents a second-generation NO sensor. When two DATI ligands are connected via a methylene chain, the dissociative fluorescence enhancement is retained while the ligand components remain intact. Although this system does not exhibit reversible NO binding, the design idea provides the possibility of creating such a desirable sensor property in the future. These results offer a paradigm for NO sensor designs, the selective displacement of a fluorescent moiety from the metal center upon NO binding.

Experimental Section

General Considerations. Tetrahydrofuran (THF), diethyl ether, and pentane were purified by passage through columns of alumina under N_2.[68] Dichloromethane (CH_2Cl_2), chlorobenzene, and triethylamine (Et_3N) were distilled from CaH_2 under N_2. 2-(Tosyloxy)tropone,[69] H-*i*-Pr_2ATI,[70] 2,2′-(pentamethylenediamino)bis(2,4,6-cycloheptatrien-1-one) ("4-dimer-tropolone"),[36] [Co(CH_3CN)$_4$](PF_6)$_2$,[71] HBAr′$_4$·2Et_2O[72] and [Co(DATI-4)] (**19**)[32] were prepared as described in the literature. Nitric oxide (Matheson, 99%) and ^{15}NO (Aldrich, 99%) were purified of higher nitrogen oxides by passage through a column of NaOH pellets and a mercury bubbler and kept over mercury in gas storage bulbs. Analysis by GC of the NO used in the experiments revealed no contaminants, such as NO_2 or N_2O, at the limit of the thermal conductivity detector, about 30 nM. All other reagents were obtained commercially and not further purified. Silica gel 60 (230−400 mesh, EM Science) or activated basic alumina (150 mesh, Brockmann I) was used for column chromatography. UV−visible spectra were recorded on a Hewlett-Packard 8435 spectrophotometer. Standard IR spectra were recorded on a Bio-Rad FTS-135 instrument; solid samples were prepared as pressed KBr disks and solution samples were prepared in an airtight Graseby-Specac solution cell with CaF_2 windows. In situ IR sample monitoring was performed with a ReactIR 1000 instrument from ASI Applied Systems equipped with a 1-in.-diameter, 30-reflection silicon ATR (SiComp) probe optimized for maximum sensitivity. Reaction protocols were as described previously.[67] Fluorescence emission spectra were recorded at 25 ± 1 °C on a Hitachi F-3010 fluorescence spectrophotometer. Mass spectra were determined in a 3-nitrobenzyl alcohol matrix with a Finnegan 4000 mass spectrometer using 70-eV impact ionization. Melting points were measured on a Thomas-Hoover capillary melting point apparatus. NMR spectra were recorded on a Bruker AC 250-MHz or a Varian Mercury 300-MHz spectrometer at ambient probe temperature and referenced to the internal ^{1}H and ^{13}C solvent peaks.

Synthetic Procedures. 2-((4-Methoxybenzyl)amino)tropone (1). To a 150-mL ethanol slurry of 2-(tosyloxy)tropone (21 g, 76 mmol) were added via syringe Et_3N (12.5 mL, 90 mmol) and (4-methoxybenzyl)amine (11.9 mL, 90 mmol). The mixture was heated to reflux under Ar. The green solution obtained within 1.5 h turned golden yellow after another 3 h. Solvents were removed by rotary evaporation, and the solid residue was treated with aqueous $NaHCO_3$, extracted into CH_2Cl_2 (3×), and dried over $MgSO_4$. Filtration and evaporation yielded a brownish crystalline solid, which was stirred in 50 mL of diethyl ether for 0.5 h and isolated by filtration to give 16.1 g (88%) of **1** as a mustard yellow, microcrystalline powder. TLC: R_f = 0.20 (5:1 hexane/ethyl

(68) Pangborn, A. B.; Giardello, M. A.; Grubbs, R. H.; Rosen, R. K.; Timmers, F. J. *Organometallics* **1996**, *15*, 1518−1520.
(69) Doering, W. v. E.; Hiskey, C. F. *J. Am. Chem. Soc.* **1952**, *74*, 5688.
(70) Dias, H. V. R.; Jin, W.; Ratcliff, R. E. *Inorg. Chem.* **1995**, *34*, 6100−6105.
(71) Goldstein, A. S.; Drago, R. S. *Inorg. Chem.* **1991**, *30*, 4506−4510.
(72) Brookhart, M.; Grant, B.; Volpe, A. F. J. *Organometallics* **1992**, *11*, 3920−3922.

acetate + 10% Et_3N, SiO_2). ^1H NMR (300 MHz, C_6D_6): δ 7.70 (1H, br s, NH), 7.36 (1H, d, J = 11.7 Hz), 6.85−6.75 (3H, m), 6.71−6.63 (3H, m), 6.22 (1H, t, J = 9.5 Hz), 6.08 (1H, d, J = 10.2 Hz), 3.79 (2H, d, J = 6 Hz), 3.26 (3H, s). IR (KBr, cm^{-1}): 3310, 2962, 2907, 1602, 1545, 1505, 1394, 1358, 1249, 1172, 1028, 854, 834, 767, 734, 668, 408. Mp: 98−100 °C. HRMS (FAB (+)), *m*/*z*: calcd for $C_{15}H_{15}NO_2$, 241.1103; found, 241.1108(7).

***N*-((4-Methoxybenzyl)amino)-2-(isopropylamino)troponimine (2).** Under an N_2 atmosphere, finely divided Me_3OBF_4 (5.62 g, 38 mmol) was added to a 75-mL CH_2Cl_2 solution of **1** (8.3 g, 34 mmol), and the mixture was stirred for 2 h. The resulting dark golden solution was chilled over an ice−water slush bath, and a portion of isopropylamine (6.4 mL, 41 mmol) was added via syringe to give a clear, red solution, which was then stirred for 2 h. Aqueous $NaHCO_3$ was added, the layers were separated, and the organic phase was dried over Na_2CO_3. Filtration and evaporation yielded a brownish yellow oil, which was recrystallized from diethyl ether at 0 °C to give 6.36 g (66%) of **2** as a yellow powder. TLC: R_f = 0.5 (5:1 hexane/ethyl acetate + 10% Et_3N, SiO_2). ^1H NMR (250 MHz, C_6D_6): δ 7.22 (2H, d, J = 8.5 Hz), 6.80 (2H, d, J = 8.6 Hz), 6.71−6.58 (2H, m), 6.32 (1H, d, J = 11.0 Hz), 6.22−6.09 (2H, m), 4.35 (2H, s), 3.61−3.51 (1H, m), 3.30 (3H, s), 1.03 (6H, d, J = 6.3 Hz). IR (KBr, cm^{-1}): 2962, 1591, 1512, 1380, 1302, 1250, 1174, 1118, 1031, 945, 828, 815, 747, 701, 540. Mp: 50−52 °C. HRMS (FAB (+)), *m*/*z*: calcd for $C_{18}H_{22}N_2O$, 282.1732; found, 282.1729(9).

***N*-((4-Methoxybenzyl)amino)-2-(*tert*-butylamino)troponimine (3).** Finely divided Me_3OBF_4 (5.1 g, 35 mmol) was added to a 50-mL CH_2Cl_2 solution of **1** (7.93 g, 33 mmol), and the mixture was stirred for 2 h under N_2. The resulting dark golden solution was chilled over an ice−water slush bath, and a portion of *tert*-butylamine (7.6 mL, 73 mmol) was added via syringe to give a dark, red-brown solution, which was stirred for 4 h. Aqueous $NaHCO_3$ was added, the layers were separated, and the organic phase was dried over Na_2CO_3. Filtration and evaporation yielded a brown solid, which was recrystallized from CH_2Cl_2/diethyl ether to give 4.91 g (50%) of **3** as a yellow, crystalline solid. TLC: R_f = 0.3 (5:1 hexane/ethyl acetate + 10% Et_3N, SiO_2). ^1H NMR (300 MHz, C_6D_6): δ 8.49 (1H, br s, NH), 7.39 (2H, d, J = 8.7 Hz), 6.92−6.87 (2H, m), 6.75−6.53 (3H, m), 6.40 (1H, d, J = 9.9 Hz), 6.16 (1H, t, J = 9.2 Hz), 4.52 (2H, s), 3.53 (3H, s), 1.19 (9H, d, J = 7.5). IR (KBr, cm^{-1}): 3201, 2969, 2832, 1611, 1588, 1459, 1368, 1284, 1229, 1174, 1032, 924, 859, 814, 770, 698, 558, 518. Mp: 103−105 °C. HRMS (FAB (+)), *m*/*z*: calcd for $C_{19}H_{24}N_2O$, 296.1889; found, 296.1883(9).

***N*-((4-Methoxybenzyl)amino)-2-(benzylamino)troponimine (4).** Finely divided Me_3OBF_4 (4.18 g, 28 mmol) was added to a 50-mL CH_2Cl_2 solution of **1** (6.20 g, 26 mmol), and the mixture was stirred for 2 h under N_2. The resulting dark golden solution was chilled over an ice−water slush bath, and portions of benzylamine (3.1 mL, 28 mmol) and Et_3N (3.9 mL, 28 mmol) were added via syringe to give an orange solution, which was stirred for 4 h. Aqueous $NaHCO_3$ was added, the layers were separated, and the organic phase was dried over Na_2CO_3. Diethyl ether was added after filtration to afford 6.25 g (73%) of **4** as a yellow, crystalline solid. TLC: R_f = 0.24 (5:1 hexane/ethyl acetate + 10% Et_3N, SiO_2). ^1H NMR (300 MHz, C_6D_6): δ 7.27 (2H, d, J = 7.5 Hz), 7.18−7.04 (5H, m), 6.78−6.75 (2H, m), 6.65−6.54 (2H, m), 6.26 (2H, t, J = 11.5 Hz), 6.10 (1H, t, J = 9.3 Hz), 4.32 (2H, s), 4.23 (2H, s), 2.28 (3H, s). IR (KBr, cm^{-1}): 3263, 3016, 2826, 1611, 1586, 1530, 1497, 1452, 1383, 1272, 1241, 1179, 1105, 1027, 824, 752, 729, 420. Mp: 104−106 °C. HRMS (FAB (+)), *m*/*z*: calcd for $C_{22}H_{22}N_2O$, 330.1732; found, 330.1739(9).

***N*-Amino-2-(isopropylamino)troponimine (5).** A portion of **2** (6.1 g, 21.5 mmol) was slowly added to 6 mL of rapidly stirring trifluoroacetic acid chilled over an ice−water slush bath. The resulting red solution was stirred for 4 h with slow warming to ambient temperature. The reaction was quenched with ice, and the sample was treated with 20 mL of aqueous 2 M NaOH and extracted into $CHCl_3$ (3×). The brown solution was dried over Na_2CO_3 and filtered, and the filtrate was evaporated to a brown oil. The product was purified by flash column chromatography on alumina (3:2 hexane/ethyl acetate + 10% Et_3N; R_f = 0.25) to afford 2.57 g (88%) of **5** as a golden oil. ^1H NMR (300 MHz, C_6D_6): δ 6.58 (1H, td, J = 10.2, 1.4 Hz), 6.34 (1H, td, J = 9.9 Hz, 1.2 Hz), 6.23 (1H, d, J = 11.4 Hz), 6.03 (1H, t, J = 9.3 Hz), 5.96 (1H, d, J = 10.2 Hz), 3.41 (1H, septet, J = 6.3 Hz), 0.95 (6H, d, J = 6.3 Hz). IR (neat on NaCl plates, cm^{-1}): 3859, 3848, 2967, 2930, 1610, 1591, 1417, 1400, 1367, 1337, 1284, 1245, 1216, 1170, 1133, 941, 881, 849, 803, 750, 699. HRMS (FAB (+)), *m*/*z*: calcd for $C_{10}H_{14}N_2$, 162.1157; found, 162.1152(5).

***N*-Amino-2-(*tert*-butylamino)troponimine (6).** A portion of **3** (4.54 g, 15.31 mmol) was slowly added to 5 mL of rapidly stirring trifluoroacetic acid chilled over an ice−water slush bath. The resulting red solution was stirred for 2.5 h with slow warming to ambient temperature. The reaction was quenched with ice, and the sample was treated with 20 mL of aqueous 2 M NaOH and extracted into $CHCl_3$ (3×). The brown solution was dried over Na_2CO_3 and filtered, and the filtrate was evaporated to a brown oil. The product was purified by flash column chromatography on alumina (1:4 ethyl acetate/hexane + 10% Et_3N; R_f = 0.28) to give 1.75 g (63%) of **6** as a golden oil. ^1H NMR (300 MHz, C_6D_6): δ 7.97 (1H, br s, NH), 6.58 (1H, t, J = 10.1 Hz), 6.33−6.27 (3H, m), 6.06−5.99 (1H, m), 1.17 (9H, s). IR (neat on NaCl plates, cm^{-1}): 2976, 2834, 1612, 1590, 1539, 1503, 1467, 1415, 1398, 1368, 1359, 1294, 1235, 1212, 1135, 1060, 1034, 880, 849, 802, 774, 750, 697. HRMS (FAB (+)), *m*/*z*: calcd for $C_{11}H_{16}N_2$, 176.1313; found, 176.1318(5).

***N*-Amino-2-(benzylamino)troponimine (7).** A portion of **4** (5.45 g, 16 mmol) was slowly added to 5 mL of rapidly stirring trifluoroacetic acid chilled over an ice−water slush bath. The resulting red solution was stirred for 2.5 h with slow warming to ambient temperature. The reaction was quenched with ice, and the sample was treated with 20 mL of aqueous 2 M NaOH and extracted into $CHCl_3$ (3×). The yellow solution was dried over Na_2CO_3 and filtered, and the filtrate was evaporated to yield 2.73 g (81%) of **7** as a yellow powder. TLC: R_f = 0.16 (5:1 hexane/ethyl acetate + 10% Et_3N, SiO_2). ^1H NMR (300 MHz, C_6D_6): δ 7.17−7.04 (4H, m), 6.45 (2H, t, J = 10.4 Hz), 6.37−6.29 (1H, m), 6.11 (1H, d, J = 11.1 Hz), 6.05−5.97 (2H, m), 4.13 (2H, s). IR (KBr, cm^{-1}): 3286, 3246, 3003, 2828, 1588, 1508, 1456, 1351, 1244, 1102, 1028, 874, 808, 756, 492. Mp: 63−66 °C. HRMS (FAB (+)), *m*/*z*: calcd for $C_{14}H_{14}N_2$, 210.1157; found, 210.1163(6).

H^{i-Pr}DATI (8). A 20-mL THF solution of **5** (2.74 g, 17 mmol) was transferred via cannula under Ar to a portion of NaH (811 mg, 20 mmol, 60% dispersion in paraffin) that had been washed with hexanes and dried in vacuo. The effervescence dissipated over 1 h, and the reaction mixture was stirred for an additional 1 h. The reaction flask was placed over an ice−water slush bath, a 15-mL THF solution of dansyl chloride (5.4 g, 20 mmol) was added dropwise under Ar, and the reaction mixture was stirred overnight. The solvent was removed in vacuo to leave a dark brown residue, which was treated with aqueous $NaHCO_3$, extracted into CH_2Cl_2 (3×), and dried over Na_2CO_3. After filtration and evacuation, the brown solid was washed with 15 mL of diethyl ether (3×) and collected by filtration. The product was purified by flash column chromatography on silica gel (4:3 hexane/ethyl acetate + 10% Et_3N; R_f = 0.20) to give 1.55 g (23%) of **8** as a light orange powder. ^1H NMR (300 MHz, C_6D_6): δ 9.21 (1H, d, J = 8.7 Hz), 8.80 (1H, dd, J = 7.2, 1.5 Hz), 8.71 (1H, d, J = 11.4 Hz), 8.4−8.36 (1H, m), 7.83 (1H, br s, NH), 7.34 (1H, t, J = 8.1 Hz), 7.18−7.12 (1H, m), 6.85 (1H, d, J = 7.5 Hz), 6.73 (1H, td, J = 10.3, 1.2 Hz), 6.59 (1H, t, J = 10.2 Hz), 6.16 (1H, t, J = 9.4 Hz), 6.01 (1H, d, J = 10.8 Hz), 2.96−2.85 (1H, m), 2.49 (6H, s), 0.52 (6H, d, J = 6.3 Hz). ^{13}C NMR (75 MHz, $CDCl_3$): δ 155.2, 154.6, 151.6, 139.1, 138.9, 138.3, 130.4, 130.1, 129.3, 127.7, 127.3, 125.5, 124.3, 123.3, 121.1, 115.3, 114.8, 45.6, 44.8, 22.0. IR (KBr, cm^{-1}): 3236, 2974, 2830, 1600, 1533, 1519, 1438, 1339, 1283, 1216, 1124, 1059, 947, 871, 846, 800, 751, 737, 708, 622, 568, 532, 464. UV−vis (CH_2Cl_2) λ, nm (ϵ, M^{-1} cm^{-1}): 263 (35 400), 359 (16 500), 433 (20 500). Mp: 163−165 °C. Anal. Calcd for $C_{22}H_{25}N_3SO_2$: C, 66.81; H, 6.37; N, 10.62; S, 8.11. Found: C, 66.62; H, 6.55; N, 10.48; S, 7.96.

H^{t-Bu}DATI (9). This compound was obtained from **6** by a procedure analogous to that described for the synthesis of **8**. The product was purified by flash column chromatography on silica gel (3:2 hexane/ethyl acetate + 10% Et_3N; R_f = 0.23) to give 1.2 g (42%) of **9** as a yellow-orange, crystalline powder. Crystals suitable for X-ray crystallography were grown by slow evaporation of CH_2Cl_2. ^1H NMR (300 MHz, C_6D_6): δ 9.19 (1H, d, J = 8.7 Hz), 8.79 (1H, dd, J = 6, 1.3 Hz), 8.72 (1H, d, J = 11.1 Hz), 8.40 (1H, d, J = 8.7 Hz), 8.13 (1H, br

s, NH), 7.33 (1H, t, $J = 8.1$ Hz), 7.18−7.13 (1H, m), 6.84 (1H, d, $J = 7.5$ Hz), 6.73 (1H, td, $J = 9.98$, 1.3 Hz), 6.63−6.52 (2H, m), 6.17 (1H, t, $J = 8.4$ Hz), 2.51 (6H, s), 0.78 (9H, s). ^{13}C NMR (75 MHz, $CDCl_3$): δ 155.6, 154.6, 151.6, 139.0, 138.2, 130.3, 130.0, 129.2, 127.4, 127.3, 125.4, 124.2, 123.4, 121.1, 116.5, 114.7, 52.6, 45.6, 28.81. IR (KBr, cm^{-1}): 3197, 2981, 2788, 1598, 1518, 1275, 1223, 1190, 1123, 946, 868, 796, 770, 745, 682, 628, 598, 590, 573, 472. UV−vis (CH_2Cl_2) λ, nm (ϵ, M^{-1} cm^{-1}): 263 (36 600), 359 (17 700), 433 (21 500). Mp: 201−202 °C. Anal. Calcd for $C_{23}H_{27}N_3SO_2$: C, 67.45; H, 6.65; N, 10.26. Found: C, 67.12; H, 6.44; N, 10.13.

H^{Bz}DATI (10). This compound was obtained from **7** by a procedure analogous to that described for the synthesis of **8**. The product was purified by flash column chromatography on silica gel (2:1 hexane/ethyl acetate + 10% Et_3N; $R_f = 0.24$) to give 1.7 g (32%) of **10** as a yellow-orange powder. ^{1}H NMR (300 MHz, C_6D_6): δ 9.21 (1H, d, $J = 8.7$ Hz), 8.85 (1H, dd, $J = 8.4$, 1.3 Hz), 8.74 (1H, d, $J = 11.1$ Hz), 8.39 (1H, d, $J = 8.1$ Hz), 8.11 (1H, br s, NH), 7.32 (1H, t, $J = 8.1$ Hz), 7.20−7.16 (1H, m), 6.97−6.95 (3H, m), 6.82 (1H, d, $J = 6.9$ Hz), 6.73−6.66 (3H, m), 6.40 (1H, t, $J = 9.4$ Hz), 6.07 (1H, t, $J = 9.4$ Hz), 6.01 (1H, d, 10.8 Hz), 3.46 (2H, d, $J = 6.3$ Hz), 2.48 (6H, s). ^{13}C NMR (75 MHz, $CDCl_3$): δ 156.0, 155.2, 151.7, 139.2, 138.6, 138.5, 135.6, 130.4, 130.1, 129.5, 129.2, 128.1, 127.9, 127.5, 127.0, 126.2, 125.0, 123.4, 121.1, 115.6, 114.9, 47.3, 45.6. IR (KBr, cm^{-1}): 3276, 2939, 2825, 1601, 1524, 1434, 1346, 1228, 1211, 1125, 864, 793, 735, 620, 590, 574, 505. UV−vis (CH_2Cl_2) λ, nm (ϵ, M^{-1} cm^{-1}): 261 (34 100), 357 (16 100), 431 (20 500). Mp: 168−170 °C. Anal. Calcd for $C_{26}H_{25}N_3SO_2$: C, 70.40; H, 5.68; N, 9.47. Found: C, 70.51, H, 5.96; N, 8.87.

[Co(*i*-Pr$_2$ATI)$_2$] (11). A portion of NaH (80 mg, 2.0 mmol of a 60% dispersion in mineral oil) was washed with hexanes and added to a 15-mL yellow THF solution of H-*i*-Pr$_2$-ATI (350 mg, 1.71 mmol). Effervescence subsided after stirring under N_2 for 1 h. Anhydrous $CoCl_2$ (129.84 mg, 1.0 mmol) was added, causing the orange solution rapidly to turn dark brown. After 4 h of stirring, the solvent was removed in vacuo, the product was extracted into CH_2Cl_2, the extract was filtered, and the filtrate was dried in vacuo. Dark brown rhombic plates suitable for X-ray crystallography were grown from slow evaporation of Et_2O. Yield: 310 mg, 78%. IR (KBr, cm^{-1}): 2966, 2925, 2863, 2345, 1686, 1654, 1585, 1497, 1468, 1416, 1379, 1362, 1305, 1265, 1225, 1168, 1151, 1121, 1072, 1019, 884, 801, 766, 670, 531. UV−vis (CH_2Cl_2) λ, nm (ϵ, M^{-1} cm^{-1}): 275 (44 000), 388 (36 000), 410 (37 000). Dec: 140−145 °C. Anal. Calcd for $CoC_{26}H_{38}N_4$: C, 67.08; H, 8.23; N, 12.03. Found: C, 67.06; H, 8.28; N, 11.97.

[Co(*i*$^{-Pr}$DATI)$_2$] (12). A portion of KH (48 mg, 1.19 mmol) was added to a 10-mL THF slurry of **8** (430 mg, 1.09 mmol) under N_2. A clear, orange solution was obtained after the effervescence had subsided, about 45 min. The color immediately turned dark amber upon the addition of anhydrous $CoCl_2$ (77.6 mg, 0.60 mmol). The solvent was evacuated after 4 h of stirring, the product was extracted into CH_2Cl_2, and the extract was filtered through Celite. X-ray-quality crystals were grown from pentane diffusion into a 1:1 CH_2Cl_2/THF solution of the complex. Yield: 363 mg, 80%. IR (KBr, cm^{-1}): 2971, 2788, 1612, 1579, 1507, 1477, 1449, 1312, 1284, 1206, 1129, 1059, 867, 791, 741, 627, 569, 498, 471. UV−vis (CH_2Cl_2) λ, nm (ϵ, M^{-1} cm^{-1}): 256 (55 900), 359 (28 200). Dec: 185−188 °C. Anal. Calcd for $CoC_{44}H_{48}N_6S_2O_4$: C, 62.32; H, 5.71; N, 9.91. Found: C, 62.47; H, 5.56; N, 9.78.

[Zn(*i*$^{-Pr}$DATI)$_2$] (13). A portion of KH (22 mg, 0.56 mmol) was added to a 10-mL THF slurry of **8** (202 mg, 0.51 mmol) under N_2. A clear, orange solution was obtained after the effervescence had subsided, about 45 min. The color lightened to yellow-orange upon the addition of anhydrous $ZnCl_2$ (38.2 mg, 0.28 mmol). The workup followed the procedure described for **12**. X-ray-quality crystals were grown from diethyl ether diffusion into a chlorobenzene solution of the complex. Yield: 280 mg, 64%. ^{1}H NMR (300 MHz, C_6D_6): δ 9.34 (2H, d, $J = 8.4$ Hz), 8.36 (2H, d, $J = 7.5$ Hz), 7.90 (2H, d, $J = 8.7$ Hz), 7.73 (2H, d, $J = 10.2$ Hz), 7.27 (2H, t, $J = 8.1$ Hz), 6.68 (4H, m), 6.43 (4H, m), 6.21 (2H, d, $J = 10.0$ Hz), 5.94 (2H, t, $J = 9.0$ Hz), 3.75 (2H, m, $J = 6.6$ Hz), 2.36 (12H, s), 1.69 (6H, d, $J = 6.6$ Hz), 1.27 (6H, d, $J = 6.3$ Hz). IR (KBr, cm^{-1}): 2972, 2869, 2786, 1615, 1581, 1513, 1481, 1452, 1409, 1315, 1286, 1211, 1129, 1060, 913, 877, 855, 794, 742, 703, 683, 626, 609, 590, 570, 550, 494, 470. UV−vis (CH_2Cl_2) λ, nm (ϵ, M^{-1} cm^{-1}): 254 (59 500), 366 (29 400), 405 (14 400). Dec: 184−187 °C. Anal. Calcd for $ZnC_{44}H_{48}N_6S_2O_4 \cdot C_6H_5Cl$ (the X-ray crystal structure and the ^{1}H NMR spectrum both confirm the presence of one molecule of chlorobenzene per Zn in the material): C, 62.11; H, 5.52; N, 8.69. Found: C, 61.82; H, 5.62; N, 8.54.

[Co(*t*$^{-Bu}$DATI)$_2$] (14). The preparation of **14** followed a procedure similar to that described for **12** using KH (24 mg, 0.60 mmol), **9** (223 mg, 0.55 mmol), and $CoCl_2$ (39 mg, 0.30 mmol). X-ray-quality crystals were grown from pentane diffusion into a 1:1 CH_2Cl_2/THF solution of the complex. Yield: 107 mg, 45%. IR (KBr, cm^{-1}): 2973, 2766, 1610, 1579, 1502, 1477, 1438, 1400, 1311, 1291, 1203, 1129, 1057, 864, 787, 744, 628, 590, 570, 479. UV−vis (CH_2Cl_2) λ, nm (ϵ, M^{-1} cm^{-1}): 254 (57 700), 361 (27 300). Dec: 209−217 °C. Anal. Calcd for $CoC_{46}H_{52}N_6S_2O_4$: C, 63.07; H, 5.98; N, 9.59. Found: C, 63.36; H, 6.13; N, 9.68.

[Co(*t*^{Bz}DATI)$_2$] (15). The preparation of **15** followed a procedure similar to that described for **12** using KH (53 mg, 1.33 mmol), **10** (537 mg, 1.21 mmol), and $CoCl_2$ (86 mg, 0.67 mmol). X-ray-quality crystals were grown from pentane diffusion into a 1:1 CH_2Cl_2/THF solution of the complex. Yield: 660 mg, 60%. IR (KBr, cm^{-1}): 2948, 2827, 1609, 1576, 1508, 1452, 1407, 1314, 1288, 1212, 1128, 1058, 868, 787, 745, 697, 628, 572, 479. UV−vis (CH_2Cl_2) λ, nm (ϵ, M^{-1} cm^{-1}): 253 (59 500), 363 (27 600). Dec: 155−160 °C. Anal. Calcd for $CoC_{52}H_{48}N_6S_2O_4$: C, 66.16; H, 5.12; N, 8.90. Found: C, 66.17; H, 5.21; N, 8.52.

1,4-Bis((*N*-(4-methoxybenzyl)-*N*′-troponimino)butane (16). A portion of "4-dimer-tropolone" (10.2 g, 34 mmol) was treated with 2.1 equiv of finely divided Me_3OBF_4 (10.7 g, 72 mmol) in 100 mL of CH_2Cl_2 under an N_2 atmosphere. After the mixture was stirred overnight, a cream-colored precipitate was collected by filtration and rinsed with ether. The solid was taken up in 15 mL of $CHCl_3$, and the solution was treated with 2 M aqueous NaOH (3×). The mixture was dried over $MgSO_4$ and filtered, and the filtrate was evaporated to dryness. The resulting solid was redissolved in 200 mL of EtOH, and (4-methoxybenzyl)amine (8.62 mL, 66 mmol) was added via syringe. The reaction mixture was stirred overnight under N_2. Then the solvent volume was reduced by half in vacuo, and a light yellow precipitate was collected by filtration and washed with diethyl ether. Yield: 13.8 g, 76%. TLC: $R_f = 0.35$ (5:1 hexane/ethyl acetate + 10% Et_3N, Si_2O_3). ^{1}H NMR (250 MHz, C_6D_6): δ 7.21 (4H, d, $J = 8.5$ Hz), 6.81 (4H, d, $J = 8.5$ Hz), 6.71−6.59 (4H, m), 6.27 (2H, d, $J = 11.0$ Hz), 6.19−6.09 (4H, m), 4.32 (4H, s), 3.29 (6H, s), 3.02−2.98 (4H, m), 1.60−1.55 (4H, m). IR (KBr, cm^{-1}): 2935, 1613, 1593, 1535, 1510, 1479, 1461, 1438, 1409, 1390, 1293, 1277, 1246, 1168, 1104, 1037, 996, 883, 814, 744, 609. Mp: 126−131 °C. HRMS (FAB (+)), *m*/*z*: calcd for $C_{34}H_{38}N_4O_2$, 534.2994; found, 534.2983(17).

1,4-Bis(*N*-amino-*N*′-troponimino)butane (17). A portion of **16** (5.2 g, 9.7 mmol) was slowly added to 8 mL of rapidly stirring trifluoroacetic acid chilled over an ice−water slush bath. The resulting red solution was stirred for 6 h with slow warming to ambient temperature. The reaction was quenched with ice, the sample was treated with 20 mL of aqueous 2 M NaOH, and the mixture was extracted into 20 mL of $CHCl_3$ (3×). The brown solution was dried over Na_2CO_3, filtered, and evaporated. Recrystallization from boiling CH_2Cl_2/diethyl ether yielded 2.15 g (75%) of **17** as a light orange, microcrystalline powder. ^{1}H NMR (250 MHz, C_6D_6): δ 6.59 (2H, t, $J = 10.1$ Hz), 6.36 (2H, t, $J = 10.0$ Hz), 6.19 (2H, d, $J = 11.1$ Hz), 6.05 (2H, t, $J = 9.3$ Hz), 5.94 (2H, d, $J = 10.4$ Hz), 2.82−2.77 (4H, m), 1.40−1.35 (4H, m). IR (KBr, cm^{-1}): 3453, 3291, 2941, 1608, 1591, 1507, 1480, 1461, 1397, 1344, 1243, 1130, 1087, 1033, 876, 855, 813, 753, 697, 604. Mp: 133−141 °C. HRMS (FAB (+)), *m*/*z*: calcd for $C_{18}H_{22}N_4$, 294.1844; found, 294.1838(9).

H$_2$DATI-4 (18). To a 200-mL solution of **17** (1.00 g, 3.4 mmol) in freshly distilled THF at 4 °C was added dropwise a portion of *n*-BuLi (4.46 mL, 7.13 mmol, 1.6 M solution in hexanes), causing the yellow-orange solution to darken to brownish yellow. After 2 h of stirring, this solution was transferred dropwise via cannula to a 150-mL THF solution of dansyl chloride (2.3 g, 8.5 mmol), also at 4 °C. The resulting brown solution was dried in vacuo after 4 h, and the residue was treated with aqueous $NaHCO_3$, followed by extraction into $CHCl_3$ (3×). The

organic phase was dried over Na_2CO_3, filtered, and dried in vacuo. The brown-orange powder obtained was stirred in 50 mL of THF for 1 h, collected by filtration, and washed with 20 mL of diethyl ether (2×) to give a mustard yellow powder. The product was purified by flash chromatography on deactivated alumina (3:2 ethyl acetate/hexanes, 10% MeOH, 10% Et_3N, Si_2O_3; $R_f = 0.26$). Yield: 663 mg, 26%. ^{1}H NMR (300 MHz, $CDCl_3$): δ 8.53 (2H, d, $J = 9$ Hz), 8.43 (4H, t, $J = 8.3$ Hz), 8.11 (2H, d, $J = 11.1$ Hz), 7.99 (1H, br s, NH), 7.54 (2H, t, $J = 8.0$ Hz), 7.37−7.28 (6H, m), 7.04 (2H, d, $J = 7.5$ Hz), 6.84 (2H, t, $J = 9.6$ Hz), 6.66 (2H, d, $J = 10.8$ Hz), 3.22 (4H, m), 2.81 (12H, s), 1.58 (4H, m). ^{13}C NMR (75 MHz, $CDCl_3$): δ 155.3, 154.9, 151.6, 139.1, 138.6, 138.4, 130.2, 129.9, 129.4, 127.7, 127.3, 125.9, 124.6, 123.4, 120.8, 115.0, 114.8, 139.1, 138.6, 138.4. IR (KBr, cm^{-1}): 3280, 2937, 2790, 1600, 1516, 1476, 1433, 1358, 1285, 1199, 1129, 1093, 1061, 1044, 988, 939, 856, 794, 738, 711, 680, 623, 600, 572, 541, 491, 462. HRMS (FAB (+)), *m*/*z*: calcd for $C_{42}H_{44}N_6S_2O_4$, 760.2865; found, 760.2887(21).

[Co(NO)$_2$(^{R}DATI)] (20; a = *i*-Pr, b = *t*-Bu, c = Bz). The procedures for **20b** and **20c** were analogous to the one described here for **20a**. In a glovebox, a portion of [Co($^{i-Pr}$DATI)$_2$] (**12**) (50 mg, 0.059 mmol) was dissolved in 10 mL of wet CH_2Cl_2 (1.8 μL of H_2O, 1.8 equiv) under an N_2 atmosphere in a 25-mL flask equipped with a gastight Teflon stopcock. The resulting red-brown solution was purged with NO for 10 min. No apparent color change was detected. The flask was sealed, and the contents were stirred for 1 week, after which the solvent was evacuated to dryness and the flask was returned to the N_2-filled glovebox. The ^{1}H NMR spectrum of the crude reaction mixture exhibited resonances for H^{i-Pr}DATI along with a new set of diamagnetic resonances assigned to **20a** in a 1:1 ratio for a 75% yield. ^{1}H NMR (300 MHz, C_6D_6): δ 9.00 (1H, d, $J = 8.7$ Hz), 8.75−8.69 (1H, m), 8.54 (1H, d, $J = 7.5$ Hz), 8.40−8.32 (1H, m), 7.94 (1H, d, $J = 10.2$ Hz), 7.85 (br s, NH), 7.36−7.32 (2H, m), 6.73 (1H, d, $J = 6.9$ Hz), 6.40 (1H, t, $J = 9.5$ Hz), 6.31−6.23 (1H, m), 6.00−5.94 (1H, m), 3.43−3.35 (1H, m), 2.41 (6H, s), 0.64 (6H, d, $J = 6.0$ Hz). IR (KBr, cm^{-1}): 1826 (ν_{NO}), 1751 (ν_{NO}), 1579, 1576, 1507, 1448, 1355, 1313, 1286, 1208, 1129, 1059, 869, 790, 746, 626, 572, 496, 472. IR (CH_2Cl_2, cm^{-1}): 1838 (ν_{NO}), 1760 (ν_{NO}).

[Co(NO)$_2$(*i*-Pr$_2$ATI)] (21). A portion of **11** (36 mg, 0.077 mmol) was dissolved in 5 mL of THF in a 25-mL, thick-walled, round-bottom flask equipped with a screw-top Teflon stopcock and a sidearm for attachment to a high-vacuum manifold. The resulting red-brown solution was subjected to three freeze−pump−thaw cycles before NO gas (0.34 mmol, 4.4 equiv) was transferred under reduced pressure to the solution. Submerging the reaction flask in a liquid N_2 bath facilitated the complete transfer of NO. No apparent color change was observed. ^{1}H NMR (250 MHz, C_6D_6): δ 6.83 (2H, t, $J = 10.0$ Hz), 6.42 (2H, d, $J = 11.2$ Hz), 6.23 (1H, t, $J = 10.2$ Hz), 3.80 (2H, m, $J = 6.1$ Hz), 0.91 (12H, d, $J = 6.2$ Hz). Dark red-black crystals of **21** were grown from slow evaporation of diethyl ether in a glovebox. IR (KBr, cm^{-1}): 1810, 1734 (ν_{NO}), 1591, 1507, 1416, 1382, 1269, 1230, 1171, 1121, 1072, 966, 815, 722, 468. Because of the mixture of products (**21** and H-*i*-Pr$_2$-ATI) present, elemental analysis was not performed.

Electrochemistry. Cyclic voltammograms were recorded with an EG&G model 263 potentiostat. The standard three-electrode setup consisted of an $Ag/AgNO_3$ reference electrode (0.01 M in acetonitrile), a platinum wire auxiliary electrode, and a 1.75 mm^2 platinum disk working electrode. Samples were measured at ambient temperature under a blanket of Ar in freshly distilled THF with 0.5 M (Bu_4N)(ClO_4) as supporting electrolyte. All spectra were externally referenced to the ferrocene/ferrocenium (Cp_2Fe/Cp_2Fe^+) couple under identical conditions, for which $E_{1/2} = 133$ mV vs $Ag/AgNO_3$ in THF. Scan rate profiles were acquired for each sample, at scan speeds of 50−100 mV/s, revealing linear plots of anodic and cathodic peak currents versus the square root of the scan rate, as expected for reversible couples. The peak-to-peak ΔE_p separations were around 100 mV, similar to the value obtained for the Cp_2Fe/Cp_2Fe^+ couple under the same conditions.

X-ray Crystallography. Single crystals were mounted on quartz fibers with Paratone N (Exxon) and transferred rapidly to the −85 °C cold stream of a Bruker (formerly Siemens) CCD X-ray diffraction system with graphite-monochromatized Mo Kα radiation ($\lambda = 0.710\ 73$ Å) controlled by a pentium-based PC running the SMART software package.[73] The temperature of the crystals was maintained with a Bruker LT-2A nitrogen cryostat. The general procedures for data collection and reduction followed those reported elsewhere.[74] Empirical absorption corrections were calculated and applied by the SADABS program.[75] Structures were solved by the direct methods program XS, and refinements were carried out with XL, both part of the SHELXTL program package.[76] Non-hydrogen atoms were refined by a series of least-squares cycles. Hydrogen atoms were assigned idealized positions and given thermal parameters that were 1.2 times those of the carbon atoms to which they were attached. All structure solutions were checked for higher symmetry with the PLATON program.[77] Enantiomorph checks were carried out by using the Flack parameter refinement in the XL program.[78] A disordered molecule of CH_2Cl_2 in the structure of **12**·CH_2Cl_2 was modeled over three positions with a ratio of 20:50:30 and refined with appropriate restraints in XL.[76] In the structure of **13**·C_6H_5Cl, a molecule of chlorobenzene was modeled as disordered over two positions with a ratio of 50:50 and refined with appropriate restraints. The solvent disorder in the structure containing **15** was successfully modeled as 0.5 CH_2Cl_2 and 0.5 THF and refined with appropriate restraints. Crystallographic data for **11**, **12**, **14**, and **15** are summarized in Table 1; the data for **19** were published previously.[32] Selected bond distances and angles for **11**, **12**, **14**, **15**, and **19** are given in Table 2, and ORTEP plots showing 50% thermal ellipsoids are displayed in Figure 1 and Figures S2, S3, S5, and S6 (Supporting Information). Crystallographic data and ORTEP plots for **9** and **13** are also included as Supporting Information in Table S1 and Figures S1 and S4, respectively.

Acknowledgment. This work was supported by a grant from the National Science Foundation and a fellowship to N.S. from the Undergraduate Research Opportunity Program of MIT. B.S. thanks the Swiss National Science Foundation for postdoctoral support.

Supporting Information Available: Figures S1−S6, displaying fully labeled ORTEP diagrams for **9**, **11**, **12**, **13**, **14**, and **15**, respectively. Figures S7 and S8, showing fluorescence spectra of **8** and **13**, respectively, at varying concentrations, Figures S9 and S10, displaying fluorescence spectra of **12** after addition of H^+ and H^{i-Pr}DATI, respectively, and Figure S11, showing the fluorescence spectra of **19** after the additions of incremental amounts of NO. X-ray crystallographic files in CIF format. This material is available free of charge via the Internet at http://pubs.acs.org.

IC000344Q

(73) *SMART*, Version 5.05; Bruker AXS, Inc.: Madison, WI, 1998.
(74) Feig, A. L.; Bautista, M. T.; Lippard, S. J. *Inorg. Chem.* **1996**, *35*, 6892−6898.
(75) Sheldrick, G. M. *SADABS: Area Detector Absorption Correction*; University of Göttingen: Göttingen, Germany, 1996.
(76) Sheldrick, G. M. *SHELXL97-2: Program for the Refinement of Crystal Structures*; University of Göttingen: Göttingen, Germany, 1997.
(77) Spek, A. L. *PLATON*: *A Multipurpose Crystallographic Tool*; Utrecht University: Utrecht, The Netherlands, 1998.
(78) Flack, H. D. *Acta Crystallogr., Sect. A* **1983**, *A39*, 876−881.